An innovative method for highly-efficient fabrication of carbon fibre precursors via acrylonitrile emulsion copolymerization coupled to a chemical oscillator

Luciana Sciascia[1], Davide Lenaz[2], Andrei Rotaru[3-5], Francesco Princivalle[2], Filippo Parisi[2,3,]*

[1]Dipartimento di Scienze della Terra e del Mare (DiSTeM), University of Palermo, 90123 Palermo, Italy
[2]Department of Mathematics and Geosciences, University of Trieste, Via Weiss 2, I-34128 Trieste, Italy
[3]Tiraspol State University, Department of Chemistry, Faculty of Biology and Chemistry, Str. Drumul Viilor, Nr. 26A, Chisinau, Republic of Moldova
[4]Department of Biology and Environmental Engineering, University of Craiova, Str. A.I. Cuza, Nr. 13, 200585 Craiova, Romania
[5]Department of Chemical Thermodynamics, Institute of Physical Chemistry "Ilie Murgulescu", Romanian Academy, Splaiul Independentei, Nr. 202, 060021 Bucharest, Romania

A new synthetic protocol for the production of the carbon fibre precursor polyacrylonitrile (PAN) and its block copolymers with polyethylene glycol (PEG) is proposed here. The constant flux of radical species produced at low concentration during the oscillating Belousov-Zhabotinsky (BZ) reaction was properly exploited to initiate the radical polymerization reaction. Compared with conventional methods, this oscillating initiation decreases the probability of chain termination, thus favouring the production of high molecular weight polymers, and does not require inert atmosphere and high temperature to be produced. The solubility of the polymeric chains during the polymerization reaction was improved by adding the anionic micelle-forming surfactant sodium dodecyl sulphate (SDS). Following the initiation step, short oligomer chains are able to overcame the micellar interface, thereby reaching a favourable environment for the increasing of the polymeric chains. This strongly contribute to the increase of the molecular weight of the fibres' precursors. The synthesis was carried out by adding the monomer acrylonitrile (AN) to the unperturbed and PEG-perturbed BZ system after the onset of the oscillations, in the absence and presence of increasing amounts of the SDS surfactant. The potentiometric technique was utilized to detect the dynamics of the oscillatory reaction. Preliminarily, the response of the BZ system to the monomer addition was investigated. Additional information was provided from the study of the effect of the SDS and PEG concentration on the dynamics of the BZ reaction during AN polymerization, thus obtaining a deepening in the understanding of the BZ mechanism. The characterization of the obtained polymers and copolymers, by melting point measurements, molecular weight determinations, FTIR, XRD analyses, and thermal treatments, indicated that the proposed synthetic method produces carbon fibre precursors with high molecular weight and good thermal stability. The addition of the surfactant was revealed as a good method to improve and/or properly tune the precursor molecular weight. The proposed synthetic protocol represents a valuable alternative to conventional methods to produce high-performant precursors of carbon fibres.

Keywords: Emulsion polymerization, surfactant, Belousov-Zhabotinsky, carbon fibers, poly(acrilonitrile), poly(ethylene glycol).

***Corresponding author**: filippo.parisi@units.it

1. *Introduction*

The present paper is based on the idea to bring together two different scientific fields, *i.e.* nonlinear dynamics and material science. Concerning this issue, different studies [1–7] were performed aiming at exploiting the far-from-equilibrium behaviour to optimize the synthetic protocol of polymeric materials or to improve the properties of the obtained materials, including at the interface (Idumah & Obele 2021).

A great deal of attention was reserved to the oscillating Belousov-Zhabotinsky (BZ) reaction, consisting in the oxidation of organic molecules (such as malonic or citric acid) in the presence of a strong acid with the assistance of metal catalysts.

Although the main scheme of the mechanism was understood (see paragraph 1.1 for a brief description), researchers in the field of non-linear dynamics are still involved in the whole elucidation of the BZ oscillator and important contributions are provided from the study of the effect of additives, such as surfactant, polymers, monomers, on the dynamics of the reactions [8–15].

Following the pioneering work of Váradi & Beck [16] and Pojman et al. [17] who first showed that acrylonitrile (AN) polymerized periodically when added to the BZ reaction, several works were performed aimed at interpreting the mechanism for polymerization coupled to oscillations [4,18].

The results of these studies suggested that the radical species, produced periodically during the oscillating reaction, can initiate a reaction of radical polymerization, thus opening route to the opportunity to trade on this periodic initiation to produce the polymer polyacrilonitrile (PAN).

PAN and its block copolymers attracted broad academic and industrial interest since they are recognized as the most important and promising precursors for high-performance carbon fibres [19–24].

Traditional approaches for preparing PAN polymers and copolymers have considerable economic and ecological disadvantages [25] and require the use of toxic solvents, inert atmosphere and high temperatures [26,27].

The employment of the radical species produced periodically during the oscillating BZ reaction represents a valuable alternative to the conventional radical polymerization. The constant flux of radical initiators at low concentration allows to keep low the concentration of growing chains and, consequently, to reduce the probability of chain termination, thus producing high molecular weight PAN precursor, which is the main prerequisite for preparation of high performance carbon fibers [28–30].

Quenching of free radicals by molecular oxygen (O_2), which represents one of the most challenging problems in conventional radical polymerization processes [26,27] , is also avoided. The polymerization procedure can also affect thermal stabilization of PAN copolymers, which is recognized as one of the most important stages for preparing carbon fibers fibres [31,32].

Further control of the whole process can be obtained by performing the radical polymerization in the presence of surfactant. The emulsion polymerization process has indeed several distinct advantages. One of the most important is the possibility to obtain high molecular weight polymers with a very low polydispersion degree and high reaction rates.

Despite the quite copious literature on the mechanistic investigation of polymerization coupled to BZ reaction, a thorough evaluation of the synthetic process and of the influence of this oscillating initiation on the features of the obtained PAN polymers is still lacking. To the best of authors knowledge, no study on the polymerization and copolymerization in emulsion coupled to oscillating chemical reactions so far exists. With the aim to investigate this new synthetic process, the polymerization of the acrylonitrile and its block copolymers with the non-ionic polymer polyethylene glicole (PEG) in emulsion and exploiting initiators systems formed during the oscillating BZ reaction was then undertaken.

This way, the twofold aim to (i) provide a contribution to the elucidation of the BZ mechanism and (i) propose a synthetic procedure for the production of high performant carbon fibers precursors, is accomplished.

The choice of PEG is in line with recent literature which reports several studies on the synthesis and characterization of PEG based copolymers with interesting features [33–38]. Moreover, the influence of the PEG copolymer onto the dynamics of the BZ reaction was already explored in a previous work [9].

The synthesis of the polymers was conducted in the absence and in the presence of increasing amounts of the anionic micelle-forming surfactant sodium dodecyl sulphate (SDS) and the polymer PEG.

The effect of the AN addition to the dynamics of the BZ system was investigated. Additional information was provided from the study of the effect of the SDS and PEG concentration on the oscillating reaction during the polymerization.

The successive step consisted in the characterization of the polymers and copolymers synthesized in the different reaction media, by melting point measurements, molecular weight determinations, Fourrier-Transform Infrared Spectroscopy (FTIR), X-Ray Diffraction (XRD) analyses and thermal stabilization processes.

1.1. Belousov-Zhabotinsky reaction

The general stoichiometry of the BZ reaction has the form:

$$2BrO_3^- + 3MA + 2H^+ \rightarrow 2BrMA + 4H_2O + 3CO_2 \qquad \text{(R1)}$$

Where MA is the malonic ($CH_2(COOH)_2$) acid and BrMA is bromomalonic acid ($BrCH(COOH)_2$).

Although only a few kinds of reagents are employed to initiate the BZ reaction, the detailed reaction mechanism is quite complex because many intermediates appear during the reaction process.

One of the first proposed models, the so-called FKN, proposed by Fields, Körös and Noyes [39], consists of 10 elementary processes, as reported in Table 1.

Table 1. Reaction steps in the FKN model

FKN 1	$HBrO+Br^-+H^+\leftrightarrow Br_2+H_2O$
FKN 2	$HBrO_2+Br^-+H^+\rightarrow 2HBrO$
FKN 3	$Br^-+BrO_3^-+2H^+\leftrightarrow HBrO+HBrO_2$
FKN 4	$2HBrO_2\rightarrow BrO^{-3}+HBrO+H^+$
FKN 5	$BrO_3^-+HBrO_2+H^+\leftrightarrow 2BrO_2\cdot+H_2O$
FKN 6	$BrO\cdot 2+Ce^{3+}+H+\leftrightarrow HBrO_2+Ce^{4+}$
FKN 7	$BrO_2\cdot+Ce^{4+}+H_2O\rightarrow BrO_3^-+2H^+$
FKN 8	$Br_2+MA\rightarrow BrMA+Br^-+H^+$
FKN 9	$6Ce^{4+}+MA+2H_2O\rightarrow 6Ce^{3+}+HCOOH+2CO_2+6H^+$
FKN 10	$4Ce^{4+}+BrMA+2H_2O\rightarrow Br^-+4Ce^{3+}+HCOOH+2CO_2+5H^+$

The whole mechanism can be modelled through a relatively simple scheme, which comprises three set of reactions indicated as A, B and C.

Each of these processes has a net effect on the overall reaction. The control of the system switches back and forth between process A and B that are coupled by the third set of reactions, C.

The bromide ion is the key species in this reaction mechanism. During the reaction its concentration dictates whether process A or B is in control at a particular time.

Process A consists in the three-step (FKN1-FNK3) reduction of bromate to bromine. The net effect of Process A is a reduction in the concentration of bromide ions in the solution, according to the following net reaction:

$$BrO_3^- + 5Br^- + 6H^+ \rightleftharpoons 3Br_2 + 3H_2O \qquad \text{(A)}$$

As a result of these reactions, the bromate is reduced and the concentration of bromide eventually falls below some critical level $[Br^-]_{cr}$. At this point that the system switches to process B, that is called positive feedback of the overall reaction.

The net transformation that takes place in Process B (combination of steps FKN4-FKN8) is as follows:

$$BrO_3^- + 4Ce(III) + 5H^+ \longrightarrow HBrO + 4Ce(IV) + 2H_2O \qquad \text{(B)}$$

This overall reaction indicates a sequence that provides the autocatalytic oxidation of Ce(III) and generates $HBrO_2$ autocatalytically. At this point, for the system oscillate, a process is required which regenerates the bromide ion and reduces the metal ion catalyst back to its lower oxidation state. This is done via process C that regenerates the bromide ion via a negative feedback (inhibition) with the reduction of Ce(IV).

$$2Ce(IV) + MA(enol) + BrMA \rightleftharpoons fBr^- + 2Ce(III) + \text{other products} \qquad \text{(C)}$$

where *f* is a stoichiometric parameter that depends on the malonic/bromomalonic acid ratio.

The FKN mechanism is able to describe the fundamental processes involved in the oscillating reaction and was applied to model oscillation and other nonlinear phenomena in the BZ reaction.

In the last years, models that substantiate the principal features of the FKN mechanism and consider some subsequent experimental results were developed. Among them, one of the most efficient is a 48-steps reaction mechanism, the Marburg–Budapest–Missoula (MBM) mechanism [40]. In the present paper the MBM model was used to investigate the effect of additives on the dynamics of the BZ reaction.

2. Experimental section

2.1. Materials

$Ce(SO_4)_2 \cdot 4H_2O$ (Ce(IV)), malonic acid (MA), sodium bromate, sulfuric acid, poly(ethylene glycol) with molecular weight 2000 g mol^{-1} (PEG 2000), and acrylonitrile (AN) were of commercial analytical quality (Fluka) and were used without further purification. Sodium dodecyl sulphate (SDS) obtained from Fluka was purified by crystallization from ethanol. Stock solutions of all chemicals used were prepared by weight before use. Deionized water from reverse osmosis (Elga, model Option 3), having a resistivity higher than 1 MΩ·cm, was used to prepare all solutions.

2.2. Kinetic measurements

The reactants of the BZ reactions were mixed following the procedure reported in Sciascia et al. 2007 [8]. Briefly, appropriate aliquots of stock solutions of $NaBrO_3$, Ce(IV) in sulfuric acid, MA sulfuric acid and additives (SDS and/or PEG) at the desired concentration were added in a double walled glass reactor in order to obtain the appropriate initial concentrations of reactants. The kinetic profiles of the oscillating reaction were followed, under stirred batch condition at 25.0 ± 0.1 °C, by monitoring the redox potential as a function of time by means of a platinum electrode in combination with a $Hg/HgSO_4$ reference electrode. Data were collected through a Hewlett-Packard multimeter.

2.3. Synthesis of polymers and copolymers

The synthesis of the polymer poly(acrylonitrile) was performed by adding the monomer acrylonitrile to the BZ system after the onset of the oscillations both in absence and in presence of different amounts of the anionic surfactant SDS. For the synthesis of the copolymer with the poly(ethylene glycol) the AN was added to the BZ system perturbed with different amounts of PEG. The polymerization was allowed to proceed with stirring for 2 h. The precipitated product was filtered and washed several times with water to remove any trace of unreacted PEG or AN. Thus, the synthesized products were dissolved in dimethylsulfoxide (DMSO) and reprecipitated with water, filtered and dried at air for at least 48 h.

For heat treatment, the powder samples were heated at 50°C, 100°C, 150 ° and 200°C for 30 minutes, in an air oven with a temperature accuracy of 1 °C.

2.4. Characterization of the polymers and copolymers

The melting points of the prepared samples were measured with a capillary melting point apparatus.

The molecular weights (Mw) of the prepared samples were estimated from viscosity measurements, performed through an Ostwald viscosimeter. DMF solutions for both polymers and copolymers were used and the following equation [41] was applied:

$$[\eta] = 2.83\cdot10^{-4}\, M_w^{0.758} \qquad (1)$$

where $[\eta]$ is the intrinsic viscosity of the polymers solutions.

The FTIR spectra were recorded on a Perkin-Elmer (Spectrum BX) Spectrometer between 4800 and 800 cm^{-1} at a resolution of 0.5 cm^{-1}

The samples were crushed in an agata mortar, then, about 5 mg were ground up with 500 mg FTIR grade KBr and compressed into a pellet.

All measurements above described were carried out at constant temperature of 25.0 C.

XRD patterns were acquired at room temperature with a Philips X-ray diffractometer (PW 1729, Netherland) using Ni-filtered Cu Kα radiation with $\lambda = 0.15406$ nm, in the range of scattering angles $2\theta = 5–60°$ at the rate of 0.01 ° min^{-1}.

The current and voltage values were 40 mA and 40 kV, respectively.

The crystallite size of the laterally order domains (Lc), normal to the crystal plane (100) corresponding to the Bragg angle chosen, was estimated by the Scherrer formula as follows [42,43] :

$$L_C = \frac{k\lambda}{Bcos\vartheta} \qquad (2)$$

where λ is the wavelength of Cu Kα radiation, θ is the Bragg angle, B is the full width at half maximum intensity (FWHM) of the peak, and k is a constant 0.89.

The crystallinity (CI) was determined by Bell and Dumbleton method [42]:

$$CI = \frac{A_C}{(A_c + A_a)} \qquad (3)$$

where A_c is the integral area of crystalline zone and A_a is the integral area of amorphous zone.

A_c was calculated using straight line segments from $2\theta = 14°$ to $2\theta = 20°$ as the baseline, while the total integral area A ($A = A_c + A_a$) using straight line segments from $2\theta = 11°$ to $2\theta = 35°$ as the baseline.

3. Results and discussion

3.1. Dynamics of the emulsion polymerization of AN coupled to BZ reaction

Figure 1 shows a typical kinetic profile of the reaction of polymerization of acrylonitrile coupled to BZ reaction.

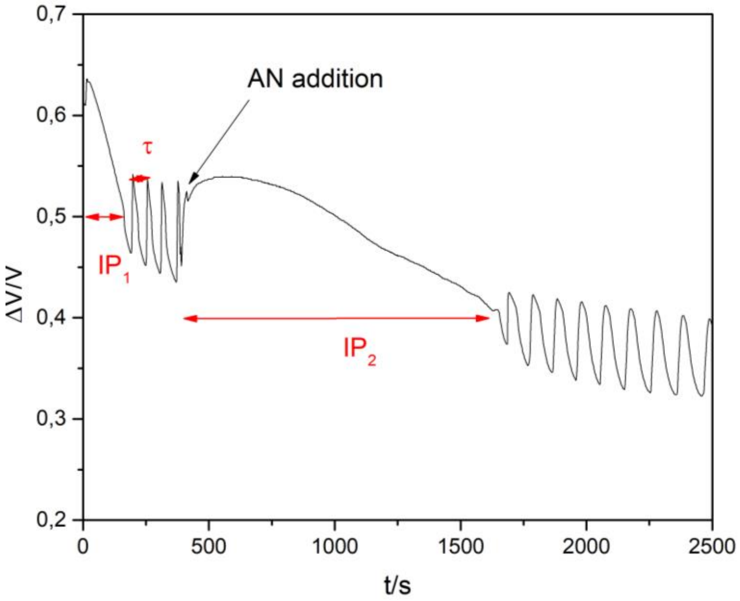

Figure 1. Potential of a Pt electrode during the BZ reaction perturbed with (a) 0.36 mol dm^{-3} of AN. $[MA]_0$ = 0.1mol dm^{-}; $[BrO_3^-]_0$=7.50 · 10^{-2} mol dm^{-3}; $[Ce(IV)]_0$ = 6.32·10^{-3} mol dm^{-3}; $[H_2SO_4]_0$ = 0.90 mol dm^{-3}; T = 25.0 °C.

As widely reported in literature [17,18], when the reactants of the BZ reaction are mixed, the potential of the solution monotonically decreases and then, after an induction period (IP_1) the system begins to oscillate with a constant oscillation period (τ). The addition of the monomer acrylonitrile inhibits oscillations and places the reaction in a high Ce(IV) quasi-steady state for a time period (second induction period, IP_2) dependent on its concentration. At the end of the IP_2 the formation of a white precipitate of polyacrylonitrile is observed. The same qualitative behaviour is observed in the presence of the surfactant SDS. The effect of the anionic surfactant on both IP_1 and τ was already discussed in Sciascia et al. 2007 [8]

Figure 2 reports the effect of AN concentration on the extent of IP_2 both in the absence and in the presence of SDS.

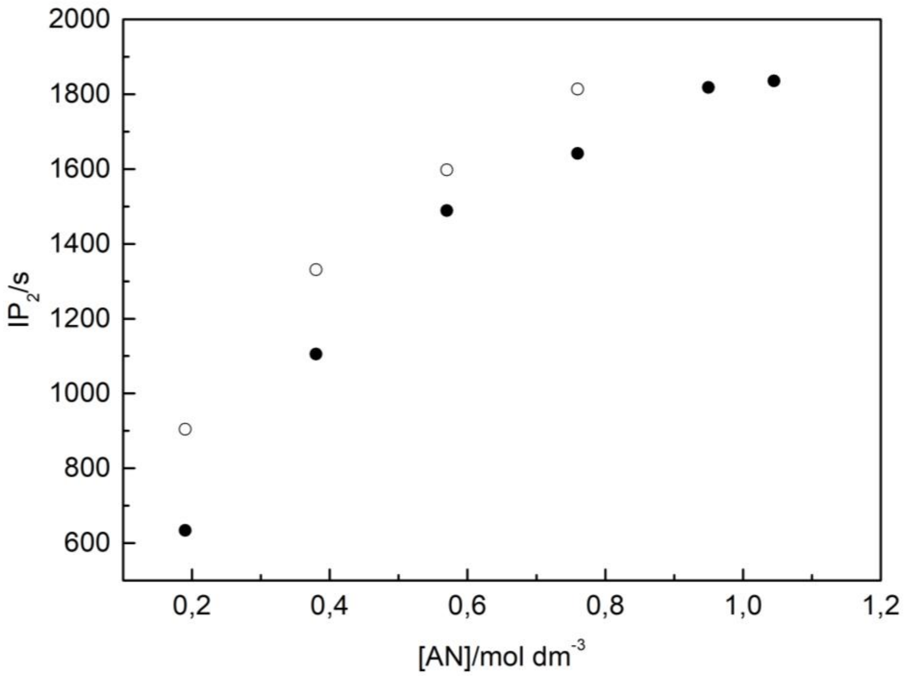

Figure 2. Plot of the second induction period (IP_2) as a function of the AN concentration for the BZ system (●) in the absence and (○) in the presence of 1.0 · 10^{-2} mol dm^{-3} of SDS. $[MA]_0$ = 0.1mol dm^{-3}; $[BrO_3^-]_0$=7.50 · 10^{-2} mol dm^{-3}; $[Ce(IV)]_0$ = 6.32·10^{-3} mol dm^{-3}; $[H_2SO_4]_0$ = 0.90 mol dm^{-3}; T= 25.0 °C.

As clearly evidenced in Figure 2, IP_2 always increases on increasing AN concentration. Moreover, it was noted that when the AN concentration reaches a critical value (0.7 mol dm^{-3} and 1.1 mol dm^{-3} in the presence and in the absence of SDS, respectively), the system is not able to start again the oscillations, at least for several hours.

The effect of acrylonitrile on the dynamics of the BZ system can be explained in the light of the reactions of polymerisation previously proposed by Washington et al.1999 and Pojman et al. 1992 [17,18]

Initiation $$MA\cdot + AN \longrightarrow P\cdot \qquad \text{(R1)}$$

Propagation $$AN + P\cdot \longrightarrow P\cdot \qquad \text{(R2)}$$

Termination $$P\cdot + P\cdot \longrightarrow P \qquad \text{(R3)}$$

$$Ce(IV) + P\cdot \longrightarrow P \qquad \text{(R4)}$$

$$BrO_2 + P\cdot \longrightarrow P \qquad \text{(R5)}$$

Because of these reactions, the reactions involving the malonic radical are hampered by the presence of the monomer AN to an extend that depend on its concentration. The reaction (MBM 32) is inhibited (the notations of the MBM model is applied [40]):

$$MA\cdot + BrO_2\cdot \longrightarrow MABrO_2 \qquad \text{(MBM 32)}$$

This implies that the availability of the radical species $BrO_2\cdot$ increases and the system require an higher concentration of BrMA to switch-off the autocatalytic cycle.

Moreover, since acrylonitrile inhibits oscillations it can be assumed that it is affecting the production of bromomalonic acid by removing HBrO and bromine from the system:

$$AN + Br_2 \longrightarrow ANBr + Br^- + H^+ \qquad \text{(R6)}$$

$$AN + HBrO \longrightarrow ANBr + H_2O \qquad \text{(R7)}$$

Since acrylonitrile subtracts HBrO and Br_2 from the reaction system, the following reactions of formation bromomalonic acid will be hampered:

$$MA + Br_2 \longrightarrow BrMA + Br^- + H^+ \qquad \text{(MBM 30)}$$

$$MA + HBrO \longrightarrow BrMA + H_2O \qquad \text{(MBM 31)}$$

The proposed mechanism is confirmed by the observation of the effect of the surfactant SDS on the dynamics of the BZ reaction during AN polymerization (Figure 3).

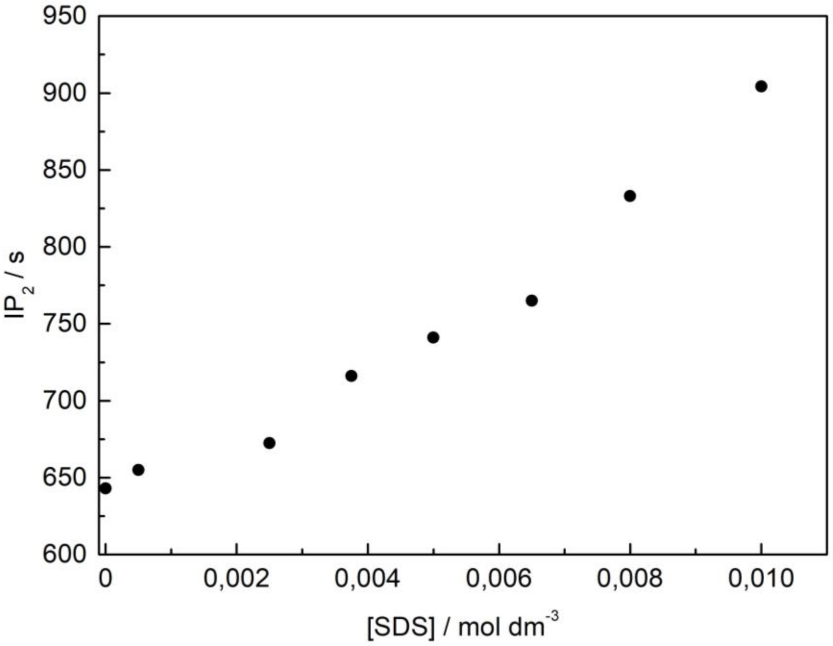

Figure 3. Plot of the second induction period as a function of surfactant concentration for the BZ system perturbed with 0.19 mol dm^{-3} of AN. $[MA]_0 = 0.1$ mol dm^{-3}; $[BrO_3^-]_0 = 7.50 \cdot 10^{-2}$ mol dm^{-3}; $[Ce(IV)]_0 = 6.32 \cdot 10^{-3}$ mol dm^{-3}; $[H_2SO_4]_0 = 0.90$ mol dm^{-3}; T = 25.0 °C.

It is worth to mention that all the experiments were performed at surfactant concentration well above the critical micellar concentration (cmc) of the SDS obtained under the experimental conditions of the BZ reaction ($3.2 \cdot 10^{-5}$ mol dm^{-3}) [8]. Therefore, the observed increase of IP_2 with SDS concentration can be attributed to the presence of the anionic micelles which favours the reactions (R6) and (R7) allowing that reactants share the same micellar pseudo-phase.

3.2. Dynamics of the emulsion copolymerization of AN with PEG coupled to BZ reaction

The synthesis of the copolymers of the polyacrylonitrile with the polyethylene glycol was performed by adding the acrylonitrile to the PEG perturbed BZ system after the onset of oscillations in absence and in presence of different amounts of the anionic surfactant SDS.

As already observed for the unperturbed BZ system, the acrylonitrile inhibits oscillations for a period indicated as second induction period, IP_2, which depends on both the polymer and the surfactant concentrations. At the end of the IP_2 the formation of a white precipitate is observed. Physical-chemical characterization of this precipitate proved that it is a copolymer of PEG and PAN (see paragraph 3.3).

The formation of the copolymer was explained by taking into account that, as reported in [9], the interaction of the polymer PEG with the BZ system leads to the formation of the polymeric radicals PEG·. As well documented in literature these radicals can initiate the vinyl polymerization of the monomer acrylonitrile:

$$PEG + AN \longrightarrow PEG - AN\cdot \tag{R8}$$

After initiation, the polymer radical can propagate consuming more acrylonitrile:

$$PEG - AN\cdot + AN \longrightarrow PEG - PAN\cdot \tag{R9}$$

Finally, the termination it is proposed to occurs throw recombination of the different radicalic polymeric chains:

$$PEG - PAN\cdot + PEG - PAN\cdot \xrightarrow{x} PEG - PAN - PAN - PEG \tag{R10}$$

$$PEG\cdot + PEG - PAN\cdot \xrightarrow{x} PEG - PAN - PEG \tag{R11}$$

$$PEG\cdot + PAN\cdot \longrightarrow PEG - PAN \tag{R12}$$

In Figure 4 the effect of the [PEG] on the IP_2 in the absence (Figure 4a) and in the presence (Figures 4 b,c,d) of three different concentrations of SDS is depicted:

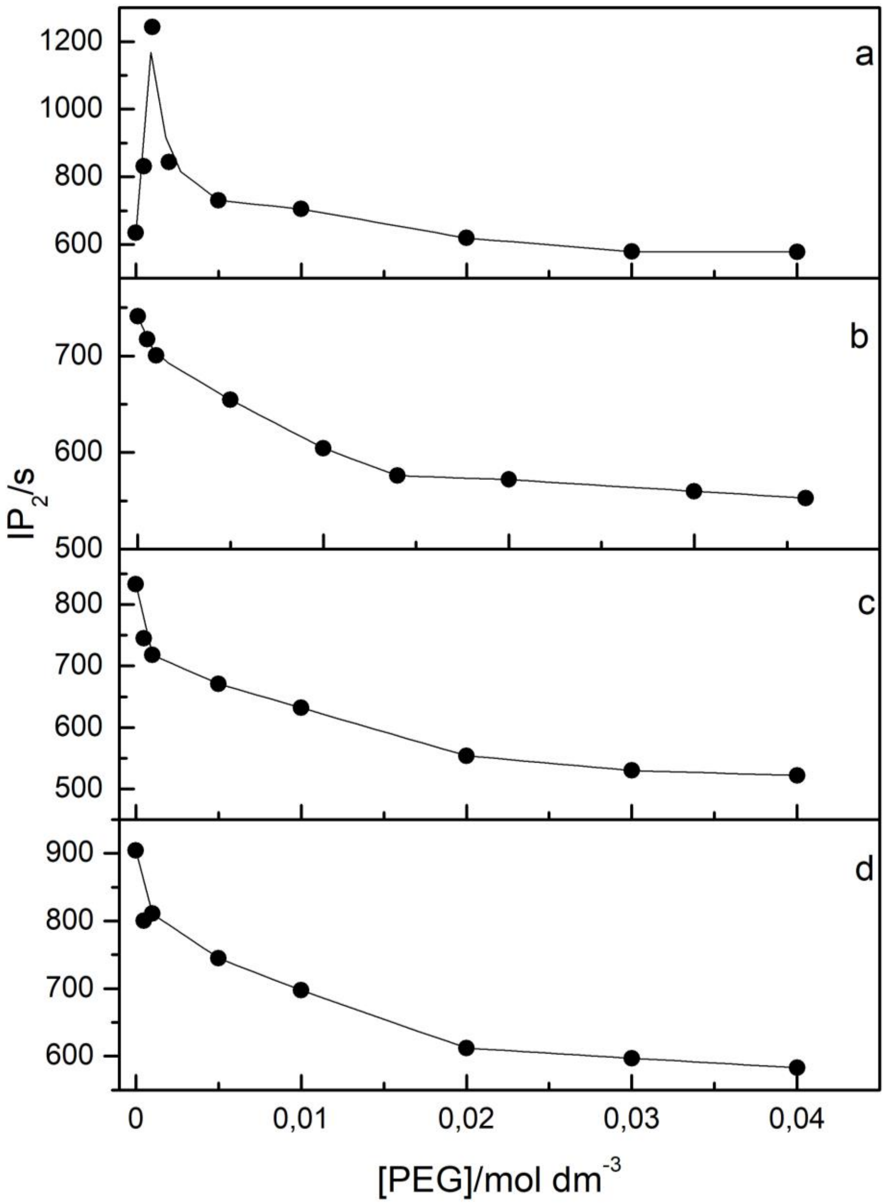

Figure 4. Plot of the second induction period (IP2) as a function of PEG-2000 for the perturbed BZ system in the absence (a), in the presence of $5.0 \cdot 10^{-3}$ mol· dm^{-3} (b), $8.0 \cdot 10^{-3}$ mol· dm^{-3} (c), $1.0 \cdot 10^{-2}$ mol· dm^{-3} of SDS. $[MA]_0 = 0.1$mol dm^{-3}; $[BrO_3^-]_0 = 7.50 \cdot 10^{-2}$ mol dm^{-3}; $[Ce(IV)]_0 = 6.32 \cdot 10^{-3}$ mol dm^{-3}; $[H_2SO_4]_0 = 0.90$ mol dm^{-3}; t = 25.0 °C

Perusal of the figure indicates that in the absence of surfactant, the IP_2 first increases and then starts to decrease on increasing PEG concentration, while, in the presence of the surfactant, it always decreases.

From a comparison with the data reported in [9], it can be noted that, the second induction period shows the same trend of the first induction period, thus indicating that the dynamic of the BZ reaction is still mainly influenced from the reactions previously proposed for the polymer effect on the IP_1. At lower PEG concentration, the reactions involving the polymeric chain of the PEG, dominates leading to an increase of the IP_2, while, at higher PEG concentration, the reactions involving the alcoholic end-groups are responsible for the decrease of the induction period. Moreover, it can be proposed that the reactions of formation of the copolymers contribute to the decrease of the IP_2. In fact, the occurrence of the reaction (R8) inhibits the reaction (R1) between malonic acid and acrylonitrile leading to an increase of the availability of the malonic acid that can scavenge the autocatalytic species $BrO_2\cdot$.

The presence of the surfactant micelles seems to inhibit the reactions of the polymer chains, probably due to the partition of the Br_2 [8].

3.3. Polymers characterization

3.3.1. Melting point measurements

The thermal analysis of the PAN homopolymers showed that, in agreements with literature data [44], poly(acrylonitrile) decomposed before melting.

As for the PAN-PEG copolymers prepared under the different experimental conditions, melting point values in the range 135-145°C were measured, while the value observed for a commercial sample of PEG was 62 °C, in agreement with literature. The shift in temperature is indicative of block copolymer formation. As a further proof, it was observed that a mixture of pure PEG and PAN homopolymers does not showed shifts in the melting point.

3.3.2. *FT-IR characterization*

Figure 5 shows the FT-IR spectra of the homo-PEG (a), homo-PAN(b), a mixture of the two copolymer (c) and the copolymer PAN-PEG :

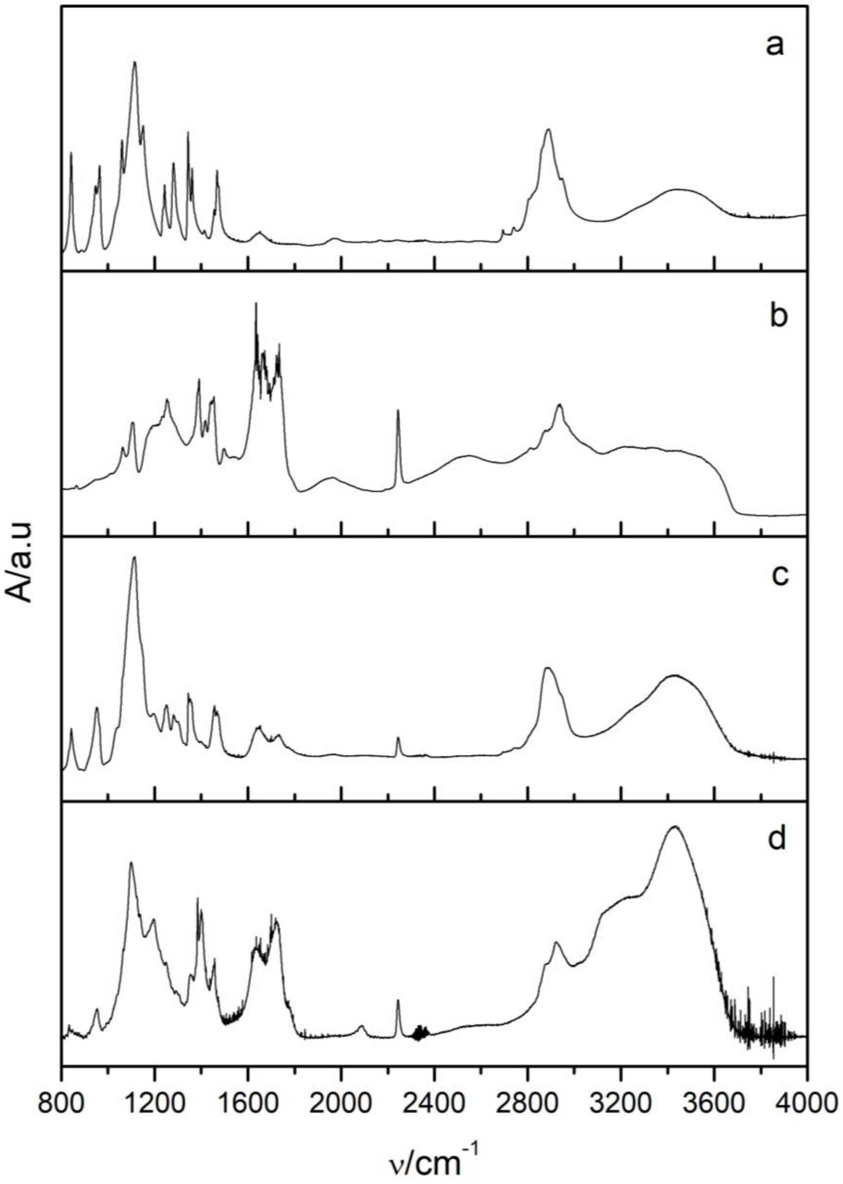

Figure 5. Fourier-Transform IR spectra of (a) homo-PEG, (b) homo -PAN, (c) mixture of the two homo-polymers and (d) block copolymer.

Examination of the Figure 5b indicates the presence of the peaks typical of the PAN structure. The peak at 2243 cm^{-1} is a clear indication of the presence of the CN group. The two peaks at 1065 and 1105 cm^{-1} can be assigned to the stretching C- C, the rocking of the methylene groups, the vibration of the C-C-CN and to the bending of the C-H. Moreover the absorption band from 1130 and 1335 cm^{-1} has been attributed to conjugate unsaturation, to C=N, C-N groups and to C-H$_{wag}$, CH$_{2wag}$ and C-C$_{stret}$. Finally, the two bans at 2000 and 2530 cm^{-1} seems to be due to the presence of H_2O adsorbed on the analysed samples.

Perusal of the Figure 5d indicates that the FT-IR spectrum of the copolymer shows peaks corresponding to both PEG and PAN. The absorption band at 3450 cm $^{-1}$ can be assigned to the terminal hydroxyl groups of the PEG segment. The bands at 2950 cm^{-1} and 1400 cm^{-1} are due to the C-H_{str} and C-H_{def} of oxyethylene group respectively. Absorption at 1125 cm^{-1} is due to C-O_{str} of PEG chain. A sharp peak at 2260 cm^{-1} corresponding to C≡N_{str} is a clear indication of the presence of PAN segment in the block copolymer. Finally, a comparison between the spectra (c) and (d), especially in the fingerprint zone, clearly distinguishes the copolymer from the mixture of its homopolymers, thus confirming the formation of the block copolymers. Moreover, it is worth to note that the procedure of preparation of the copolymers does not allow for the presence of homo-PEG in the precipitated samples, because this polymer has a high solubility in water. Therefore, it is possible to exclude that the samples are constituted from a mixture of the two polymers.

3.3.3. Molecular weight determination

The viscosity-average molecular weight (Mw) of the PAN homopolymers obtained under the different conditions was determined viscometrically.

The following figure shows the effect of the monomer concentration on the molecular weight of the obtained polymers.

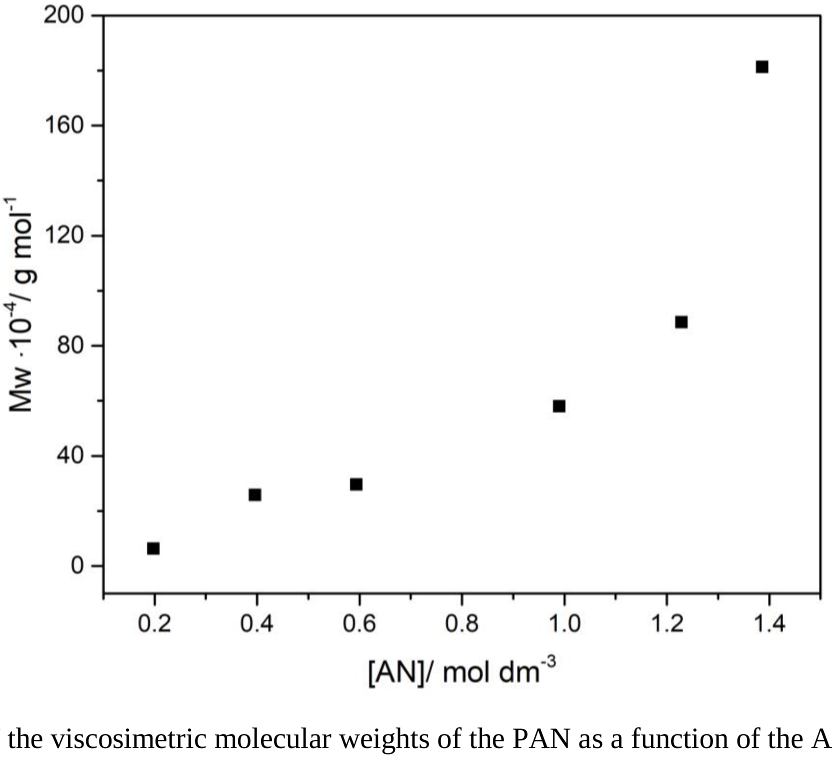

Figure 6. Plot of the viscosimetric molecular weights of the PAN as a function of the AN concentration.

Perusal of figure 6 shows that the molecular weight of the PAN polymers is affected from the initial concentration of the monomer, and it increases on increasing AN concentration. This trend can be easily explained by considering that an increase of the AN concentration will favour the reactions of propagation of the polymeric chain. This way, the polymers can reach higher molecular weights before the reaction of terminations occurs.

Figure 6 shows that the effect of the anionic surfactant SDS on the molecular weight values of the obtained polymers is different on varying the AN concentration:

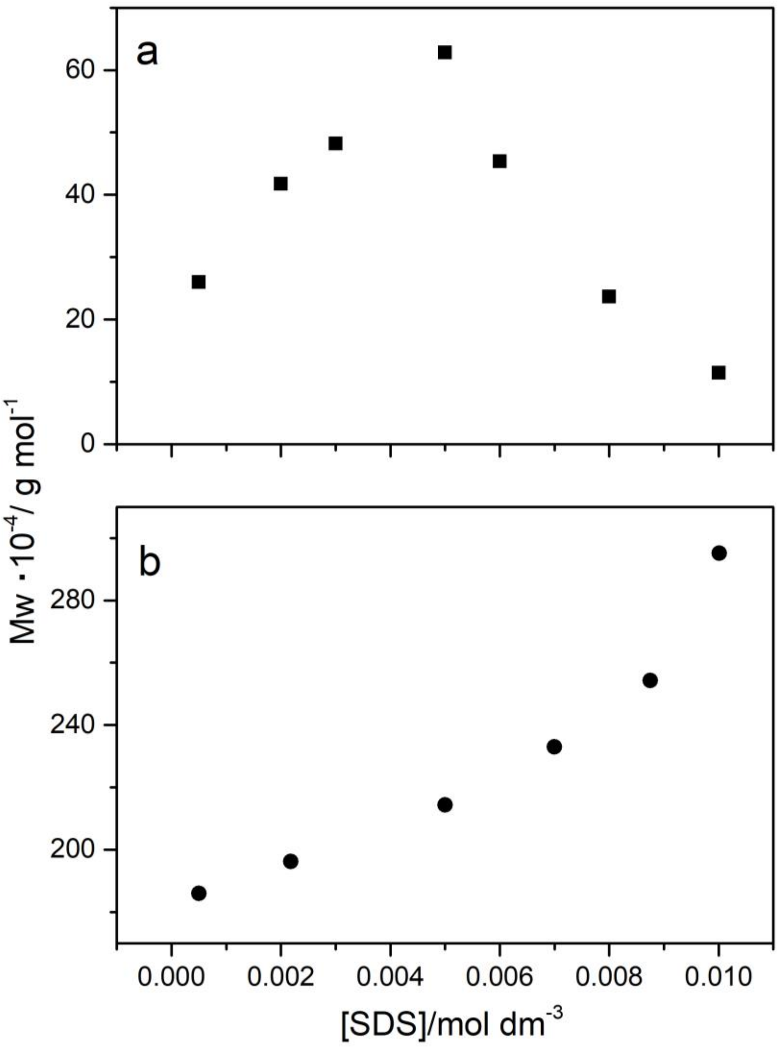

Figure 6. Plot of the viscosimetric molecular weights of the PAN obtained from (a) 0.19 mol dm^{-3} and (b) 0.95 mol dm^{-3} of AN, as a function of the SDS concentration

It was found that at the lowest AN concentration the molecular weight of the polymers first increases on increasing SDS concentration and then starts to decrease.

The increase of the molecular weights may be due to the better environment that the anionic micelle of the surfactant offers to the polymer chain growing process. Such trend was previously observed [45] for AN polymerization with other redox systems.

On the other hand, the decrease of the Mw at the highest SDS concentrations can be explained in the light of the interactions between the aggregates system and the species involved in the reactions (R6) and (R7). In fact, since both the monomer acrylonitrile, then the brominated species Br_2 and HBrO, is confined into the micellar core of the micelles, the rate of the above-mentioned reactions are enhanced. This will decrease the concentration of the monomer AN available for the reactions of polymerization. This explanation is confirmed from the observation that at higher AN concentration the negative effect of the SDS became negligible.

The surfactant concentration at which the Mw trend shows the discontinuity point coincides with the sphere-to-rod transition concentration reported in Sciascia et al. [8].

It is worth to note that the molecular weights of the polymers obtained with this new synthetic method are comparable or higher than those obtained with the other current approaches [41,46,47]. Moreover it has been observed that, unlike conventional methods , this way of synthesis can be carry out in the presence of air and at room temperature [26,27].

As for the PEG-PAN copolymers, it was found that the molecular weight values of the copolymers are greater than that of the homopolymer of PAN. This is the results of the increase of the water solubility of the polymeric radicals during the process of lengthening the polymer chain due to the presence of the hydrophilic segment of the PEG. Moreover, Figure 7 shows that the molecular weight of the copolymers is affected by the initial concentration of the polymer PEG and since it increases on increasing PEG concentration.

Bearing in mind that, according to the water solubility of the PEG homopolymer, the precipitated samples cannot contain this polymer, the dependence of the molecular weight on the PEG concentration further confirm their copolymeric nature. In fact, if the sample was just the homopolymer PAN, there should be no effects of the PEG concentration on the molecular weight.
The increase of the molecular weight on increasing PEG concentration can be reasonably explained in the light of the increase of the PEG· radicals' concentration which favours the reactions of chain propagation.

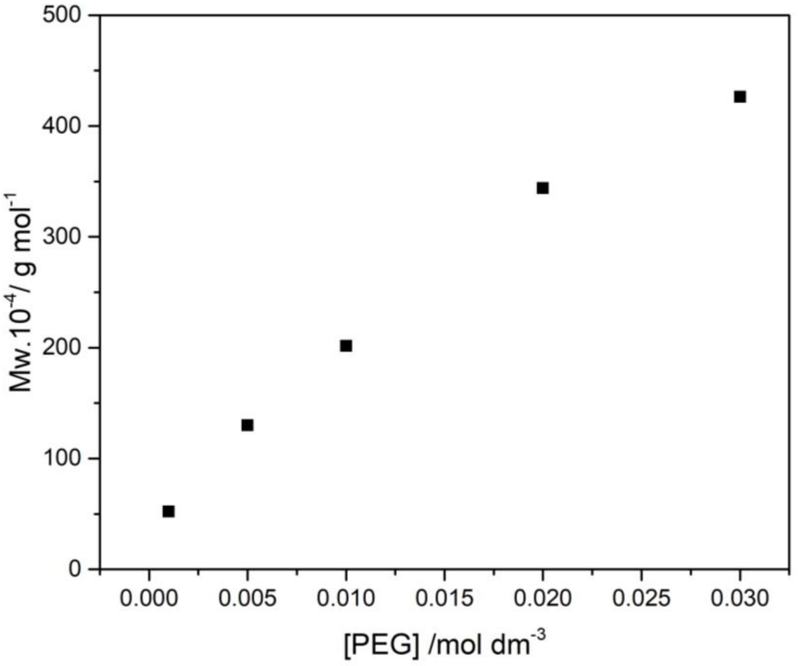

Figure 7. Plot of the viscosimetric molecular weights of the PAN-PEG copolymer synthesized as a function of the PEG concentration.

Figure 8 shows that, the molecular weights of the copolymers first increase on increasing SDS concentration and then start to decrease.

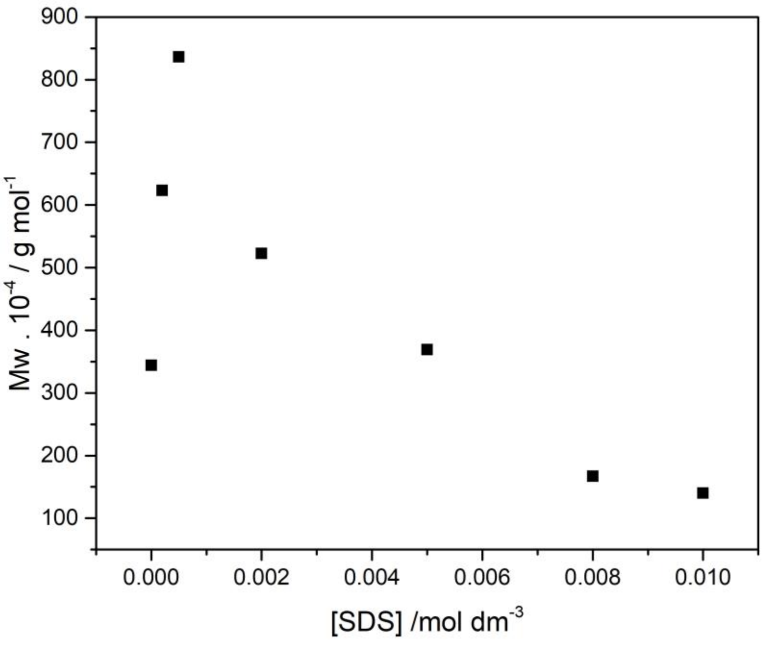

Figure 8. Plot of the viscosimetric molecular weights of the PAN-PEG copolymer synthesized in the presence of 0.02 mol dm^{-3} of PEG as a function of the SDS concentration.

The increase of the molecular weight may be due to the better environment provided by the micellar aggregates for the lengthening of the polymeric chain. The decrease at higher SDS concentrations is the results of the strong interaction between the polymeric backbones of the PEG and the anionic micelles, which inhibits the production of the polymeric radicals PEG·, leading to a decrease of the molecular weight. The above results showed that both the polymer and the surfactant concentrations affect the molecular weight of the obtained polymers, so that the correct choice of the concentrations of these two additives allows for the modulations of the molecular weight of the products.

3.3.4. XRD characterization

Typical XRD patterns of the PAN polymers and copolymers, prepared in the presence and in the absence of SDS, are presented in Figure 9.

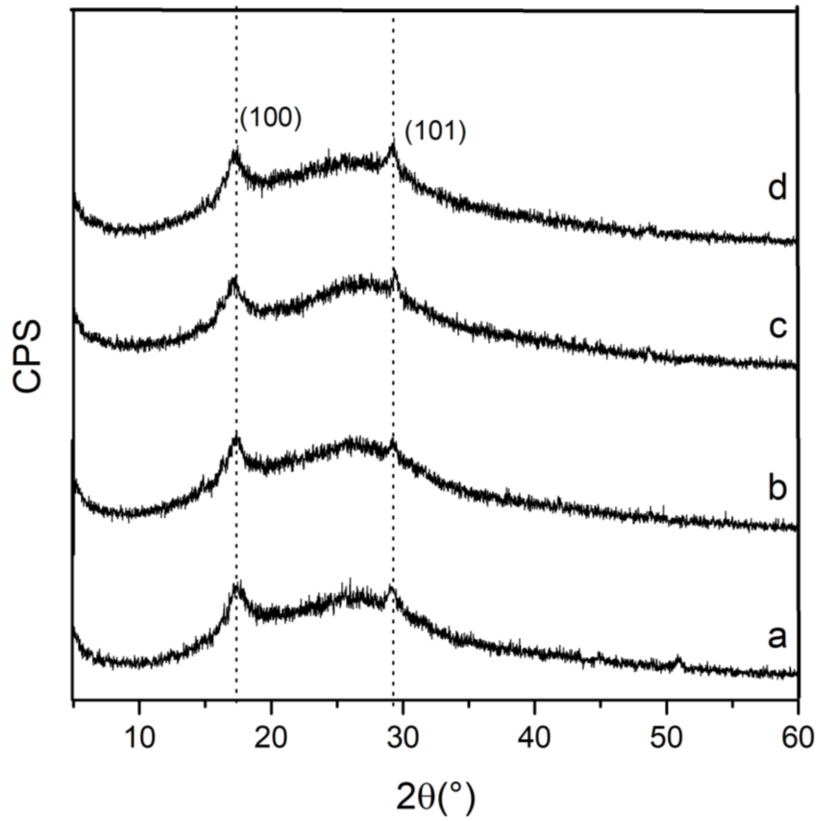

Figure 9. XRD patterns of PAN polymer prepared (a) in the absence and (b) in the presence of SDS, and PAN/PEG copolymers prepared (c) in the absence and (d) in the presence of SDS.

The characteristic diffraction peaks at about 2θ ~17 ° and 2θ ~ 29 ° correspond to (100) and (101) crystalline planes of the pseudohexagonal cell, while the broad peak around 2θ~25° comes from the amorphous region [21,48].

The peak at 2θ ~17 ° was analyzed to calculate the interplanar distance of the (100) planes (d), the crystallite size (Lc) and the degree of crystallinity (CI), through Eq. 1 and Eq. 2 (Table 2)

Table 2. Crystalline parameters of PAN and PEG/PAN powder samples.

Sample name *	**Peak (°)**	**d(Å)**	**FMWH (°)**	**Lc (Å)**	**CI (%)**	**Mw·10^{-4}(g mol^{-1})**
PAN	17,6	5,0	1,6	49.7	25,5	6,26
PAN_s	17,4	5,0	0,85	94.2	24,6	11,42
PEG/PAN	17,3	5,1	0,71	112.9	24,6	344
PEG/PAN_s	17,4	5,1	0,84	94.6	24,9	140

***The subscript "_s " stands for "prepared in the presence of surfactant"**

The presence of the polymer PEG determines an increase of the crystallite size, which may be attributed to the large volume of PEG. Analogous results were obtained for the b-methylhydrogen itaconate (MHI) in Ju et al. [49]. As expected, the values of the crystallite size follow the same trend of the molecular weight values (see the values of Mw reported in table 2 for the analyzed samples).

The crystallinity index values are well inside the range between 10 and 80%, usually observed for PAN polymers which indicates that PAN polymers crystallized PAN polymers often exist in semi crystalline state [50],

The CI values are not affected from the presence of both polymer PEG and surfactant SDS, thus suggesting that the presence of the PEG polymer does not disrupt the regular macromolecular structure of the fiber precursor.

To study the effect of heating temperature on stabilization of the prepared polymers and copolymers, the powder samples were stabilized at different temperatures (namely 50, 100, 150 and 200°C) for 30 min and their XRD patterns were recorded.

Figure 10 reports the results obtained in the case of PAN polymers. Analogous results were obtained in the case of the polymers and copolymers prepared in the absence and presence of SDS.

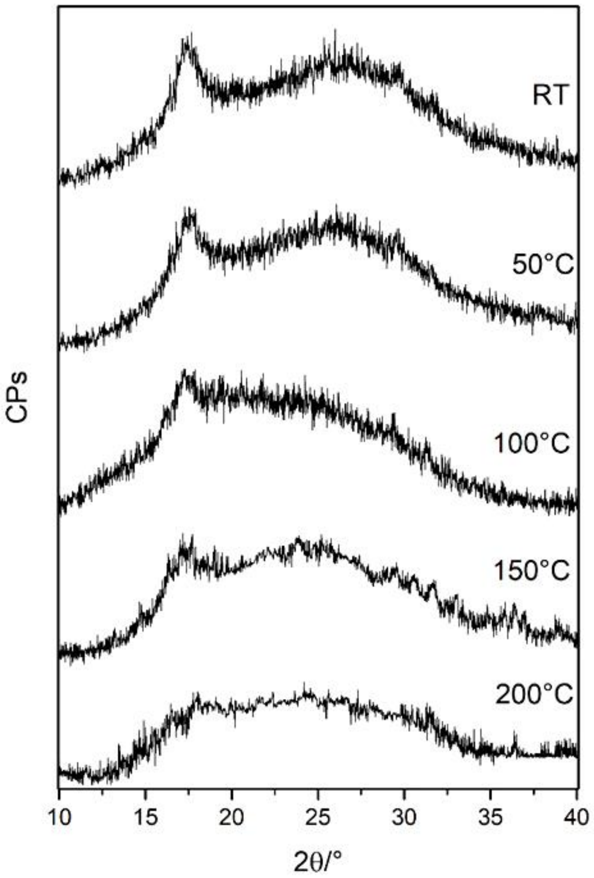

Figure 10. XRD patterns of PAN polymer stabilized at different temperatures

The changes on the XRD patterns, due to the heating treatments, are the consequence of the stabilization process converting the linear polymeric structure to a ladder structure, which could keep fibers infusible and nonflammable when carbonized at higher temperatures [32]. The structural changes during the stabilization agree well with the intensity changes of the peak around 2θ ~ 17°. Thus, the peak intensities of the peaks around 2θ ~ 17° were used to calculate the extent of stabilization (Stabilization Index, S_I), reported in Table 3, through the following formula in Eq. 4 [32]:

$$S_I = \frac{(I_0 - I_S)}{I_S} \times 100 \tag{4}$$

where I_0 is the intensity of peak around 2θ ~ 17° from the original polymer, and I_s is the intensity from the polymer stabilized for 30 min.

Table 3. Stabilization Index (S_I) results for PAN and PEG/PAN powder samples

	PAN		**PAN_s**		**PEG/PAN**		**PEG/PAN_s**	
Heat treatment temperature (°C)	**I (CPs)**	**SI (%)**	**I (CPs)**	**SI (%)**	**I (CPs)**	**SI (%)**	**I (CPs)**	**SI (%)**
RT	402	**0**	421	**0**	410	**0**	428	**0**
50	390	**3**	425	**-1**	400	**2**	430	**0**
100	405	**-1**	415	**1**	406	**1**	435	**-2**
150	196	**51**	200	**55**	222	**47**	250	**44**
200	77	**80**	85	**84**	90	**80**	86	**85**

When the heating temperature is lower than 150°C, the stabilization has not yet started, the SI is almost null. When the heating temperature is T≥150 °C, the peak intensity of 2θ ~ 17° starts to decrease significantly, thus confirming the polymer chains convert from linear to ladder structure.

It could be highlighted that the stabilization process starts at lower temperature as compared to typical results data reported in literature [19,49].

4. Conclusions

A novel synthetic procedure for the production of high-performant carbon fibre precursors, i.e poly(acrilonitrile) (PAN) and its bock copolymers with poly(ethylene glycol) (PEG), was here successfully tested.

Radical emulsion polymerization of acrylonitrile (AN) was carried out by using the anionic micelle-forming surfactant sodium dodecyl sulphate (SDS) for the emulsification and the radical species, produced during the oscillating Belousov-Zhabotinsky (BZ) reaction as initiators.

Preliminarily, the response of the BZ system to the perturbant (AN, SDS, and PEG) additions was investigated, thus obtaining a deepening in the understanding of the BZ mechanism.

The characterization of the obtained polymers and copolymers, by melting point measurements, molecular weight determinations, FTIR, XRD analyses, and thermal treatments, indicated that the proposed synthetic procedure allow to overcome common drawbacks related to conventional methods to produce carbon fibre precursors with high molecular weight and good thermal stability.

5. References

[1] W. Harmon Ray, C.M. Villa, Nonlinear dynamics found in polymerization processes — a review, Chem. Eng. Sci. 55 (2000) 275–290. https://doi.org/10.1016/S0009-2509(99)00323-1.
[2] J.A. Pojman, Q. Tran- Cong- Miyata, Introduction, in: J.A. Pojman, Q. Tran- Cong- Miyata (Eds.), Nonlinear Dyn. Polym., 1st ed., Wiley, 2010: pp. 1–4. https://doi.org/10.1002/9783527632602.ch1.
[3] J.A. Pojman, Nonlinear Chemical Dynamics In Synthetic Polymer Systems, in: P. Borckmans, P. De Kepper, A.R. Khokhlov, S. Métens (Eds.), Chemomechanical Instab. Responsive Mater., Springer Netherlands, Dordrecht, 2009: pp. 221–240. https://doi.org/10.1007/978-90-481-2993-5_9.
[4] Y. Furue, K. Okano, T. Banno, K. Asakura, Controlled polymerization of acrylonitrile proceeded along with the Belousov–Zhabotinsky oscillator by changing its stirring conditions, Chem. Phys. Lett. 645 (2016) 210–214. https://doi.org/10.1016/j.cplett.2015.12.045.
[5] B.P. Bastakoti, J. Perez-Mercader, Autonomous Ex Novo Chemical Assembly with Blebbing and Division of Functional Polymer Vesicles from a “Homogeneous Mixture,” Adv. Mater. 29 (2017) 1704368. https://doi.org/10.1002/adma.201704368.
[6] A. Osypova, M. Dübner, G. Panzarasa, Oscillating Reactions Meet Polymers at Interfaces, Materials. 13 (2020) 2957. https://doi.org/10.3390/ma13132957.
[7] I. Berlanga, Synthesis of Non-Uniform Functionalized Amphiphilic Block Copolymers and Giant Vesicles in the Presence of the Belousov–Zhabotinsky Reaction, Biomolecules. 9 (2019) 352. https://doi.org/10.3390/biom9080352.
[8] L. Sciascia, R. Lombardo, M.L.T. Liveri, Nonlinear Response of a Batch BZ Oscillator to the Addition of the Anionic Surfactant Sodium Dodecyl Sulfate, J. Phys. Chem. B. 111 (2007) 1354–1360. https://doi.org/10.1021/jp067052g.
[9] L. Sciascia, F. Rossi, C. Sbriziolo, M.L.T. Liveri, R. Varsalona, Oscillatory dynamics of the Belousov–Zhabotinsky system in the presence of a self-assembling nonionic polymer. Role of the reactants concentration, Phys. Chem. Chem. Phys. 12 (2010) 11674. https://doi.org/10.1039/c003033c.
[10] F. Rossi, R. Lombardo, L. Sciascia, C. Sbriziolo, M.L.T. Liveri, Spatio-Temporal Perturbation of the Dynamics of the Ferroin Catalyzed Belousov−Zhabotinsky Reaction in a Batch Reactor Caused by Sodium Dodecyl Sulfate Micelles, J. Phys. Chem. B. 112 (2008) 7244–7250. https://doi.org/10.1021/jp8003739.
[11] L. Onel, M. Wittmann, K. Pelle, Z. Noszticzius, L. Sciascia, The Source of the Carbon Monoxide in the Classical Belousov−Zhabotinsky Reaction, J. Phys. Chem. A. 111 (2007) 7805–7812. https://doi.org/10.1021/jp073512+.
[12] I. Berenstein, D. Barragán, Additive effects of methyl ketones in the Belousov-Zhabotinsky reactions, J. Braz. Chem. Soc. 15 (2004) 844–848. https://doi.org/10.1590/S0103-50532004000600010.
[13] F. Rossi, M. Rustici, C. Rossi, E. Tiezzi, Isotopic Effect on the Kinetics of the Belousov-Zhabotinsky Reaction, Int. J. Mol. Sci. 8 (2007) 943–949. https://doi.org/10.3390/i8090943.
[14] K. Pelle, M. Wittmann, Z. Noszticzius, R. Lombardo, C. Sbriziolo, M.L. Turco Liveri, Perturbation of the Oscillatory BZ Reaction with Methanol and Ethylene Glycol: Experiments and Model Calculations, J. Phys. Chem. A. 107 (2003) 2039–2047. https://doi.org/10.1021/jp026713g.
[15] S. Lateef, N.B. Ganaie, G.M. Peerzada, Perturbation on dynamics of ferroin-catalyzed Belousov–Zhabotinsky reaction by monomer N-isopropylacrylamide and poly(N-isopropylacrylamide), Polym. Bull. 79 (2022) 2777–2798. https://doi.org/10.1007/s00289-021-03660-7.
[16] Z. Váradi, M.T. Beck, Inhibition of a homogeneous periodic reaction by radical scavengers, J Chem Soc Chem Commun. (1973) 30–31. https://doi.org/10.1039/C39730000030.

[17] J.A. Pojman, D.C. Leard, W. West, Periodic polymerization of acrylonitrile in the cerium-catalyzed Belousov-Zhabotinskii reaction, J. Am. Chem. Soc. 114 (1992) 8298–8299. https://doi.org/10.1021/ja00047a055.

[18] R.P. Washington, W.W. West, G.P. Misra, J.A. Pojman, Polymerization Coupled To Oscillating Reactions: (1) A Mechanistic Investigation of Acrylonitrile Polymerization in the Belousov−Zhabotinsky Reaction in a Batch Reactor, J. Am. Chem. Soc. 121 (1999) 7373–7380. https://doi.org/10.1021/ja990743o.

[19] H. Chen, Y. Pan, S. Hou, Z. Shao, Y. Hong, A. Ju, Poly(acrylonitrile- *co* -2-methylenesuccinamic acid) as a potential carbon fiber precursor: preparation and stabilization, RSC Adv. 7 (2017) 54142–54152. https://doi.org/10.1039/C7RA11548B.

[20] E. Frank, L.M. Steudle, D. Ingildeev, J.M. Spörl, M.R. Buchmeiser, Carbon Fibers: Precursor Systems, Processing, Structure, and Properties, Angew. Chem. Int. Ed. 53 (2014) 5262–5298. https://doi.org/10.1002/anie.201306129.

[21] Q. Gao, M. Jing, C. Wang, S. Zhao, M. Chen, J. Qin, Preparation of High-Quality Polyacrylonitrile Precursors for Carbon Fibers Through a High Drawing Ratio in the Coagulation Bath During a Dry-Jet Wet Spinning Process, J. Macromol. Sci. Part B. 58 (2019) 128–140. https://doi.org/10.1080/00222348.2018.1548074.

[22] G. Chen, Y. Xu, T. Shi, X. Wu, X. Zhang, R. Wen, Y. Liu, M. Fang, X. Min, Z. Huang, Preparation and properties of polyacrylonitrile/polyethylene glycol composite fibers phase change materials by centrifugal spinning, Mater. Res. Express. 6 (2019) 095502. https://doi.org/10.1088/2053-1591/ab2d0a.

[23] G. Chen, T. Shi, X. Zhang, F. Cheng, X. Wu, G. Leng, Y. Liu, M. Fang, X. Min, Z. Huang, Polyacrylonitrile/polyethylene glycol phase-change material fibres prepared with hybrid polymer blends and nano-SiC fillers via centrifugal spinning, Polymer. 186 (2020) 122012. https://doi.org/10.1016/j.polymer.2019.122012.

[24] N. Sarier, R. Arat, Y. Menceloglu, E. Onder, E.C. Boz, O. Oguz, Production of PEG grafted PAN copolymers and their electrospun nanowebs as novel thermal energy storage materials, Thermochim. Acta. 643 (2016) 83–93. https://doi.org/10.1016/j.tca.2016.10.002.

[25] A.V. Shlyahtin, I.E. Nifant'ev, V.V. Bagrov, D.A. Lemenovskii, A.N. Tavtorkin, P.S. Timashev, Synthesis of polyacrylonitrile copolymers as potential carbon fibre precursors in CO_2, Green Chem. 16 (2014) 1344–1350. https://doi.org/10.1039/C3GC41677A.

[26] F. Oytun, M.U. Kahveci, Y. Yagci, Sugar overcomes oxygen inhibition in photoinitiated free radical polymerization, J. Polym. Sci. Part Polym. Chem. 51 (2013) 1685–1689. https://doi.org/10.1002/pola.26554.

[27] S.O. Ilyin, E.V. Chernikova, Yu.V. Kostina, V.G. Kulichikhin, A.Ya. Malkin, Viscosity of polyacrylonitrile solutions: The effect of the molecular weight, Polym. Sci. Ser. A. 57 (2015) 494–500. https://doi.org/10.1134/S0965545X15040070.

[28] E.A. Morris, M.C. Weisenberger, M.G. Abdallah, F. Vautard, H. Grappe, S. Ozcan, F.L. Paulauskas, C. Eberle, D. Jackson, S.J. Mecham, A.K. Naskar, High performance carbon fibers from very high molecular weight polyacrylonitrile precursors, Carbon. 101 (2016) 245–252. https://doi.org/10.1016/j.carbon.2016.01.104.

[29] J. Kaur, L. Hillbrick, A. Abbott, P. Lynch, P. Mota-Santiago, A.P. Pierlot, High molecular weight improves microstructure and mechanical properties of polyacrylonitrile based carbon fibre precursor, Polymer. 247 (2022) 124753. https://doi.org/10.1016/j.polymer.2022.124753.

[30] Y. Xu, J. Sun, H. Chen, L. Bai, Synthesis of polyacrylonitrile by reversible-deactivation radical polymerization and its application as electrode materials for electrochemical double layer capacitors, RSC Adv. 5 (2015) 37780–37788. https://doi.org/10.1039/C5RA05651A.

[31] S. Arbab, A. Zeinolebadi, Quantitative analysis of the effects of comonomers and heating conditions on the stabilization reactions of polyacrylonitrile fibers as carbon fiber precursors, Polym. Degrad. Stab. 139 (2017) 107–116. https://doi.org/10.1016/j.polymdegradstab.2017.04.003.

[32] W. Dang, J. Liu, X. Wang, K. Yan, A. Zhang, J. Yang, L. Chen, J. Liang, Structural Transformation of Polyacrylonitrile (PAN) Fibers during Rapid Thermal Pretreatment in Nitrogen Atmosphere, Polymers. 12 (2020) 63. https://doi.org/10.3390/polym12010063.

[33] N. Sarier, R. Arat, Y. Menceloglu, E. Onder, E.C. Boz, O. Oguz, Production of PEG grafted PAN copolymers and their electrospun nanowebs as novel thermal energy storage materials, Thermochim. Acta. 643 (2016) 83–93. https://doi.org/10.1016/j.tca.2016.10.002.

[34] A. Kuru, S.A. Aksoy, Cellulose–PEG grafts from cotton waste in thermo-regulating textiles, Text. Res. J. 84 (2014) 337–346. https://doi.org/10.1177/0040517513494251.

[35] Y. Li, R. Liu, Y. Huang, Synthesis and phase transition of cellulose- *graft* -poly(ethylene glycol) copolymers, J. Appl. Polym. Sci. 110 (2008) 1797–1803. https://doi.org/10.1002/app.28541.

[36] A. Sarı, C. Alkan, A. Biçer, Synthesis and thermal properties of polystyrene-graft-PEG copolymers as new kinds of solid–solid phase change materials for thermal energy storage, Mater. Chem. Phys. 133 (2012) 87–94. https://doi.org/10.1016/j.matchemphys.2011.12.056.

[37] Q. Guo, Q. Xue, T. Wu, X. Pan, J. Zhang, X. Li, L. Zhu, Excellent dielectric properties of PVDF-based composites filled with carbonized PAN/PEG copolymer fibers, Compos. Part Appl. Sci. Manuf. 87 (2016) 46–53. https://doi.org/10.1016/j.compositesa.2016.04.008.

[38] K. Sui, L. Gu, Preparation and characterization of amphiphilic block copolymer of polyacrylonitrile-block-poly(ethylene oxide), J. Appl. Polym. Sci. 89 (2003) 1753–1759. https://doi.org/10.1002/app.12036.

[39] R.J. Field, E. Koros, R.M. Noyes, Oscillations in chemical systems. II. Thorough analysis of temporal oscillation in the bromate-cerium-malonic acid system, J. Am. Chem. Soc. 94 (1972) 8649–8664. https://doi.org/10.1021/ja00780a001.

[40] L. Hegedűs, M. Wittmann, Z. Noszticzius, S. Yan, A. Sirimungkala, H.-D. Försterling, R.J. Field, HPLC analysis of complete BZ systems. Evolution of the chemical composition in cerium and ferroin catalysed batch oscillators: experiments and model calculations, Faraday Discuss. 120 (2002) 21–38. https://doi.org/10.1039/b103432b.

[41] H. Jiang, M. Zhou, D. Pan, Synthesis of Ultra-High Molecular Weight Polyacrylonitrile (UHMWPAN) by Aqueous Suspension Polymerization, Adv. Mater. Res. 1120–1121 (2015) 615–619. https://doi.org/10.4028/www.scientific.net/AMR.1120-1121.615.

[42] Y. Zhao, C. Wang, Y. Bai, G. Chen, M. Jing, B. Zhu, Property changes of powdery polyacrylonitrile synthesized by aqueous suspension polymerization during heat-treatment process under air atmosphere, J. Colloid Interface Sci. 329 (2009) 48–53. https://doi.org/10.1016/j.jcis.2008.09.055.

[43] V.B. Gupta, S. Kumar, The effect of heat setting on the structure and mechanical properties of poly(ethylene terephthalate) fiber. I. Structural changes, J. Appl. Polym. Sci. 26 (1981) 1865–1876. https://doi.org/10.1002/app.1981.070260611.

[44] Y. Qin, A brief description of textile fibers, in: Med. Text. Mater., Elsevier, 2016: pp. 23–42. https://doi.org/10.1016/B978-0-08-100618-4.00003-0.

[45] M. Patra, A.K. Behera, R.K. Behera, B.K. Sinha, Effects of surfactants on acrylonitrile polymerization initiated by a Cr(VI)-cyclohexanone redox system: A kinetic study, J. Appl. Polym. Sci. 91 (2004) 1147–1153. https://doi.org/10.1002/app.13198.

[46] E.V. Chernikova, Z.A. Poteryaeva, S.S. Belyaev, I.E. Nifant’ev, A.V. Shlyakhtin, Yu.V. Kostina, A.S. Cherevan’, M.N. Efimov, G.N. Bondarenko, E.V. Sivtsov, Controlled synthesis of polyacrylonitrile via reversible addition-fragmentation chain-transfer pseudoliving radical polymerization and its thermal behavior, Polym. Sci. Ser. B. 53 (2011) 391. https://doi.org/10.1134/S1560090411070013.

[47] I. Grabchev, V. Bojinov, Synthesis and characterisation of fuorescent polyacrylonitrile copolymers with 1,8-naphthalimide side chains, Polym. Degrad. Stab. 70 (2000) 147–153. https://doi.org/10.1016/S0141-3910(00)00100-2.

[48] H. Zhang, L. Quan, F. Shi, C. Li, H. Liu, L. Xu, Rheological Behavior of Amino-Functionalized Multi-Walled Carbon Nanotube/Polyacrylonitrile Concentrated Solutions and Crystal Structure of Composite Fibers, Polymers. 10 (2018) 186. https://doi.org/10.3390/polym10020186.

[49] A. Ju, Y. Yan, D. Wang, J. Luo, M. Ge, M. Li, A high molecular weight acrylonitrile copolymer prepared by mixed solvent polymerization: I. effect of monomer feed ratios on polymerization and stabilization, RSC Adv. 4 (2014) 64043–64052. https://doi.org/10.1039/C4RA10779A.

[50] T.A. Adegbola, O. Agboola, O.S.I. Fayomi, Review of polyacrylonitrile blends and application in manufacturing technology: recycling and environmental impact, Results Eng. 7 (2020) 100144. https://doi.org/10.1016/j.rineng.2020.100144.

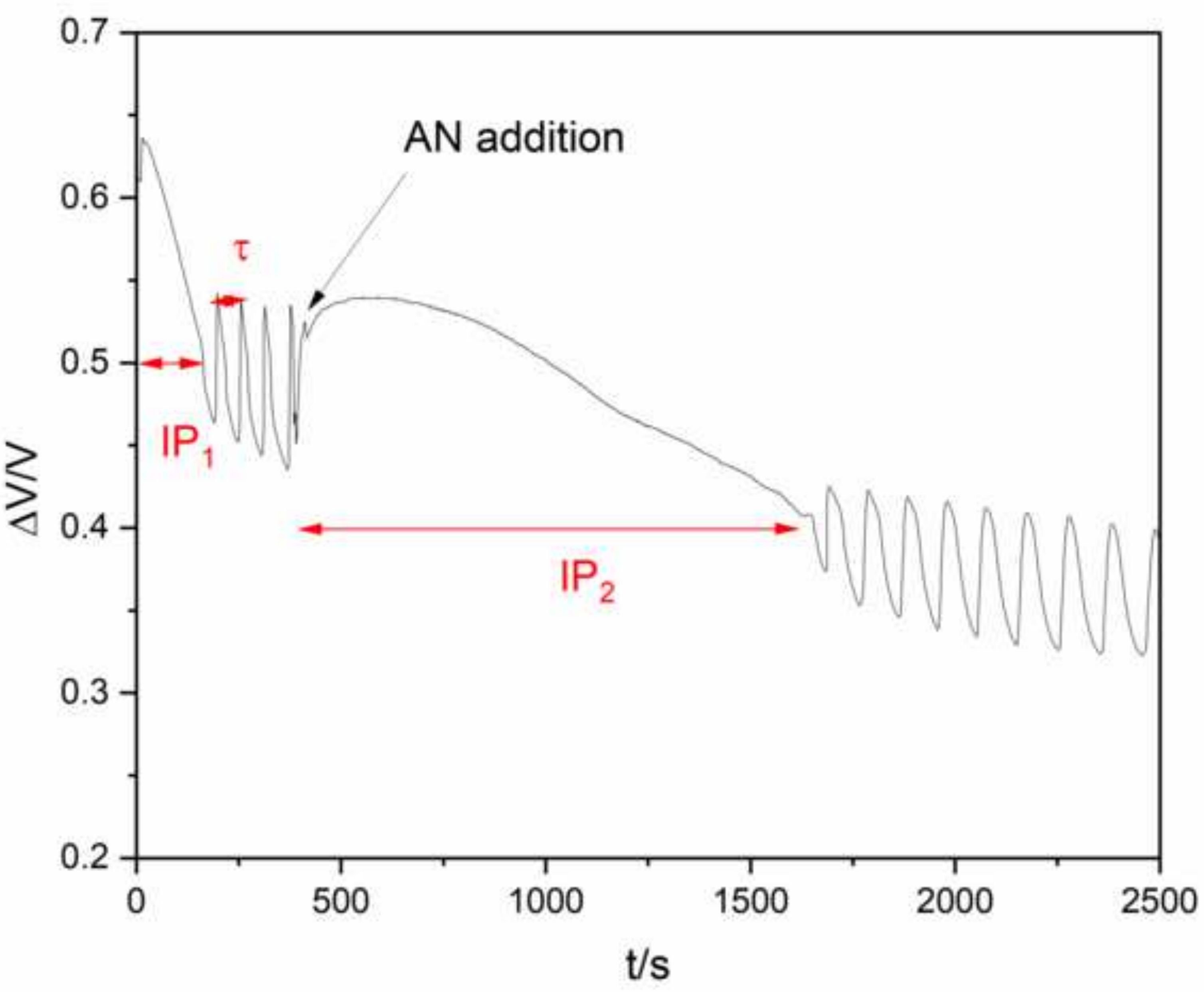
AN addition
τ
IP_1
IP_2
ΔV/V
0.7
0.6
0.5
0.4
0.3
0.2
0
500
1000
1500
2000
2500
t/s

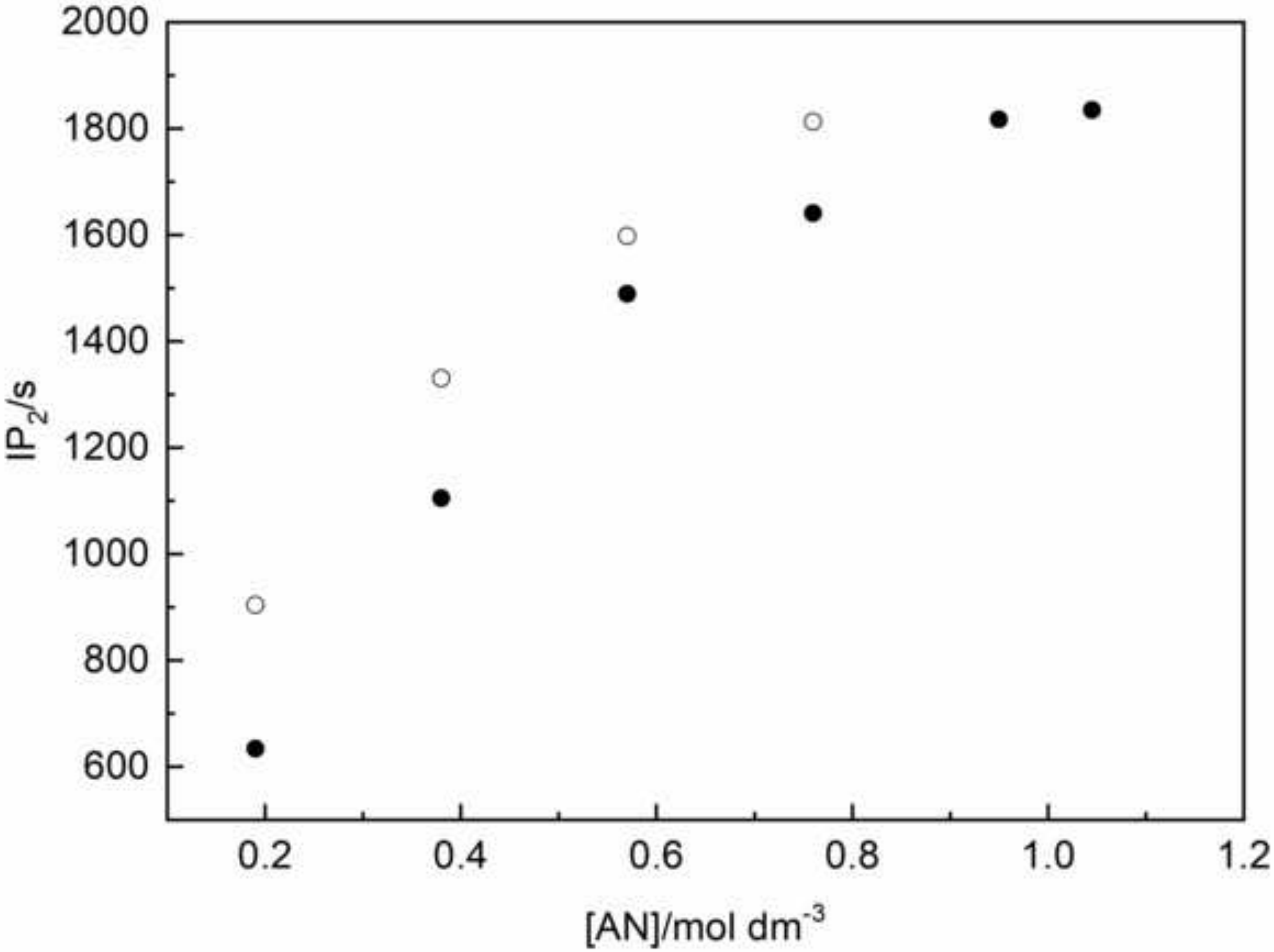
2000
1800
1600
1400
1200
1000
800
600
IP_2/s
0.2
0.4
0.6
0.8
1.0
1.2
[AN]/mol dm^{-3}

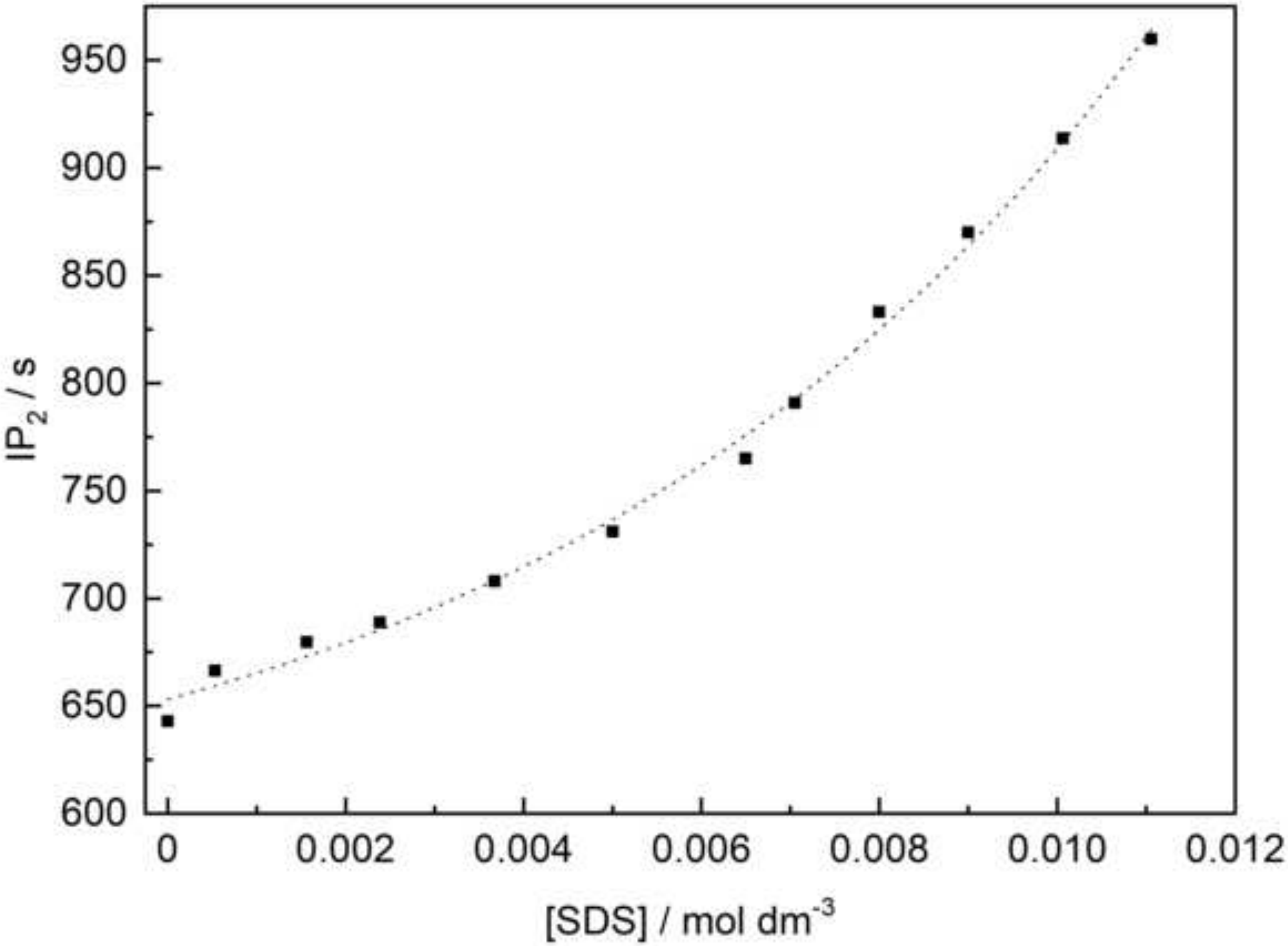

950
900
850
800
750
700
650
600
IP_2 / s
0
0.002
0.004
0.006
0.008
0.010
0.012
[SDS] / mol dm^{-3}

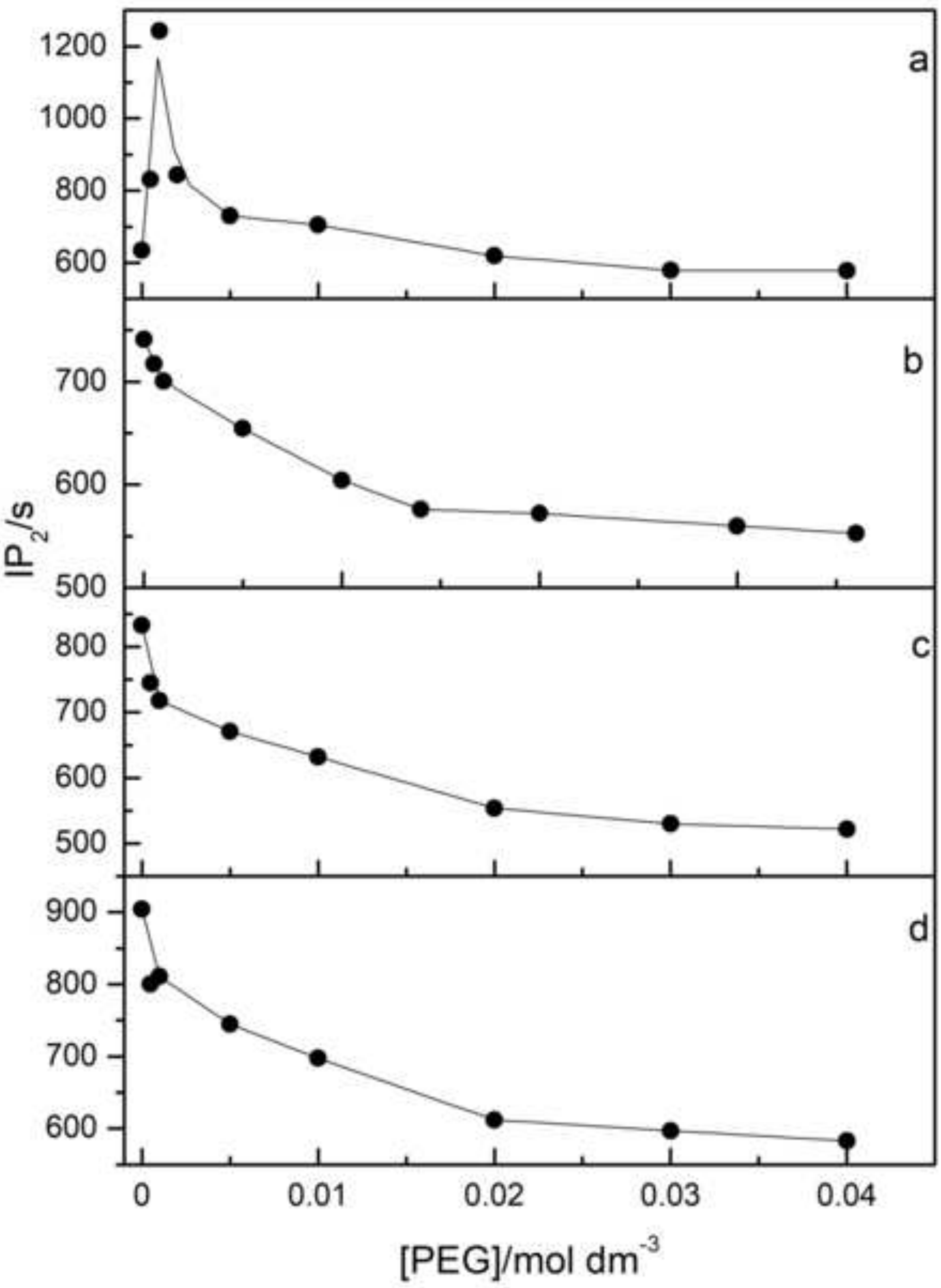
1200
1000
800
600
a
700
600
500
b
800
700
600
500
c
900
800
700
600
d
IP$_2$/s
0
0.01
0.02
0.03
0.04
[PEG]/mol dm^{-3}

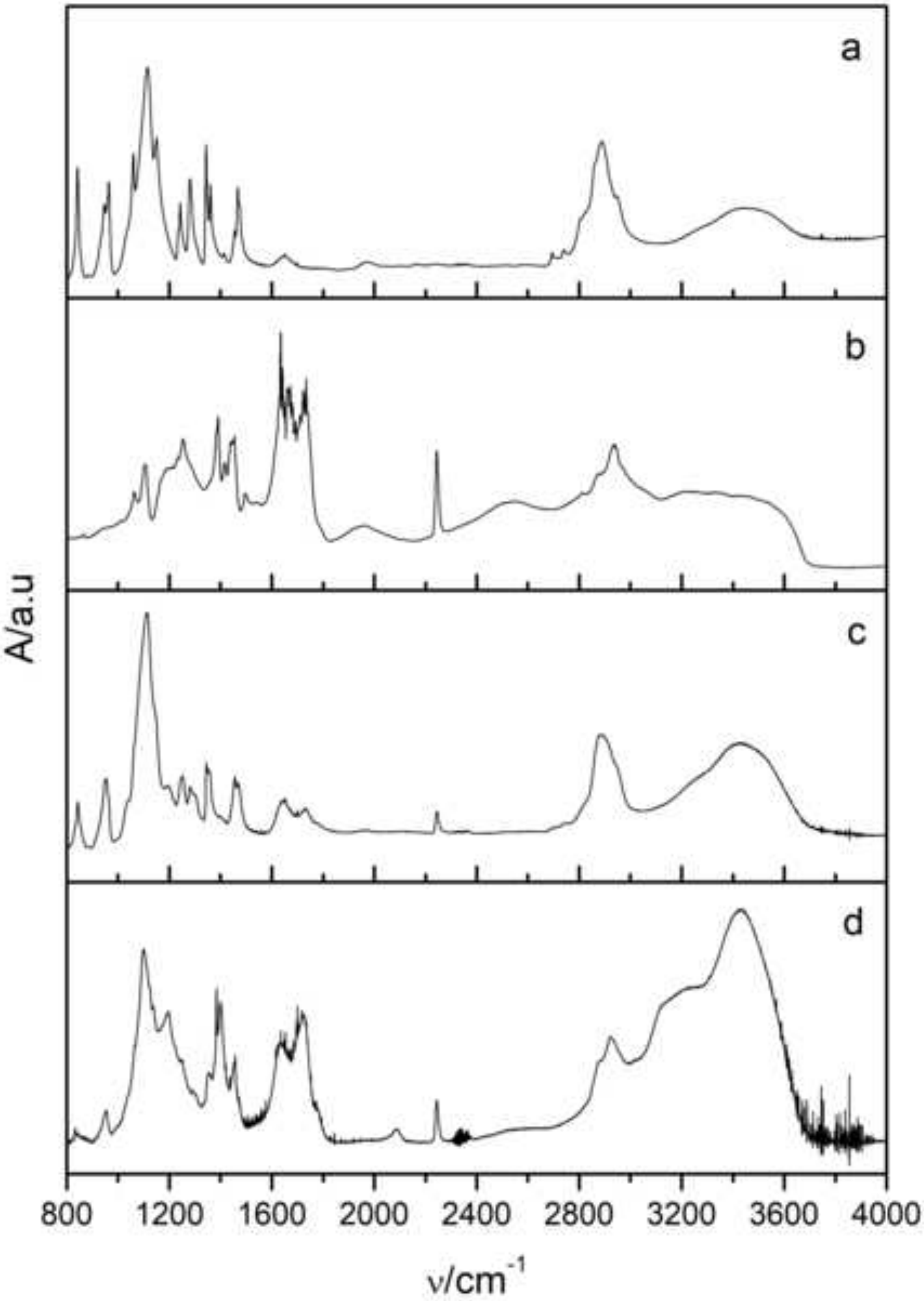
a
b
c
d
A/a.u
800
1200
1600
2000
2400
2800
3200
3600
4000
ν/cm^{-1}

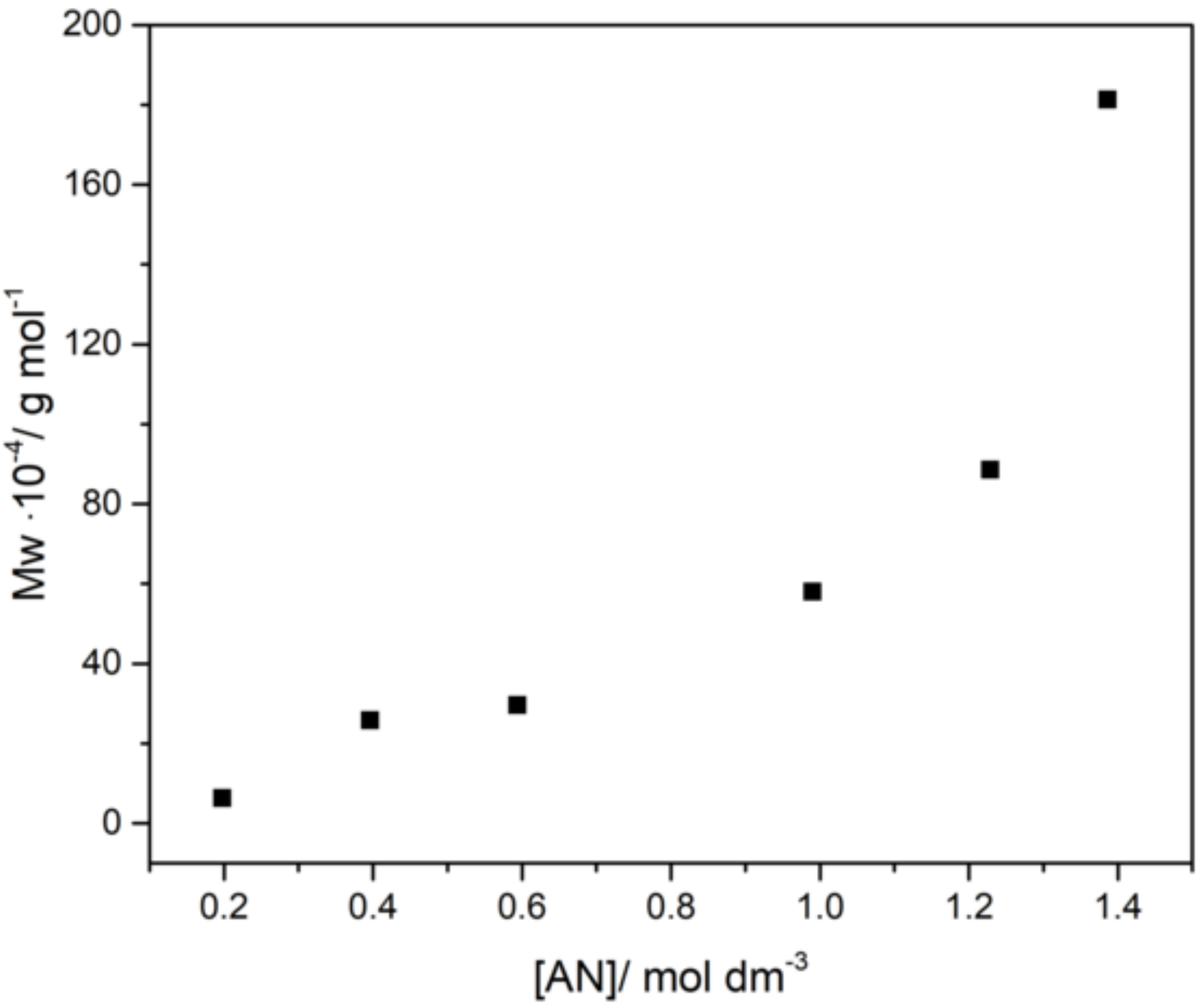
200
160
120
80
40
0
0.2
0.4
0.6
0.8
1.0
1.2
1.4
Mw ·10^{-4}/ g mol^{-1}
[AN]/ mol dm^{-3}

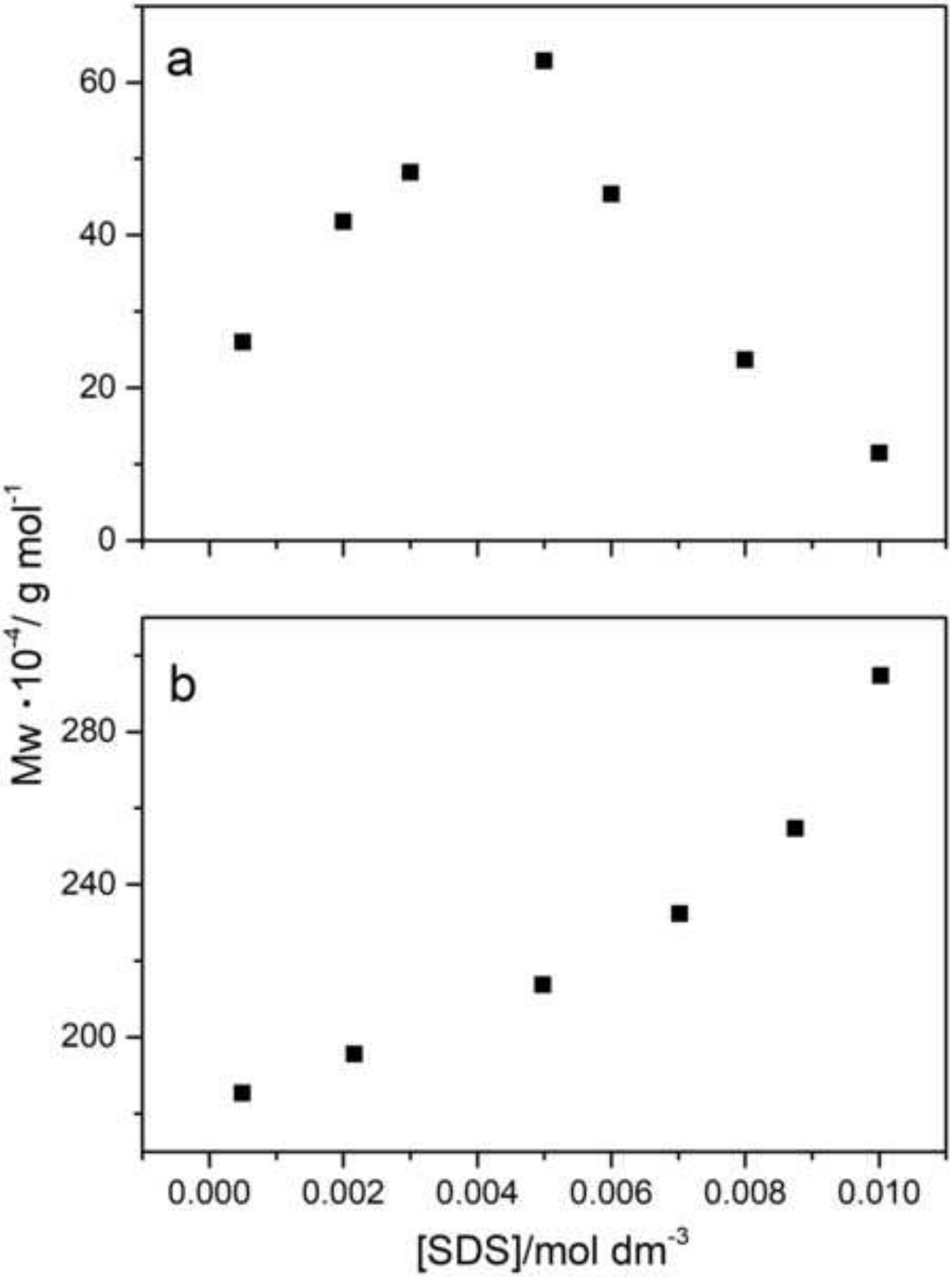
a
60
40
20
0
b
280
240
200
Mw · 10^{-4}/ g mol^{-1}
0.000
0.002
0.004
0.006
0.008
0.010
[SDS]/mol dm^{-3}

Figure 8

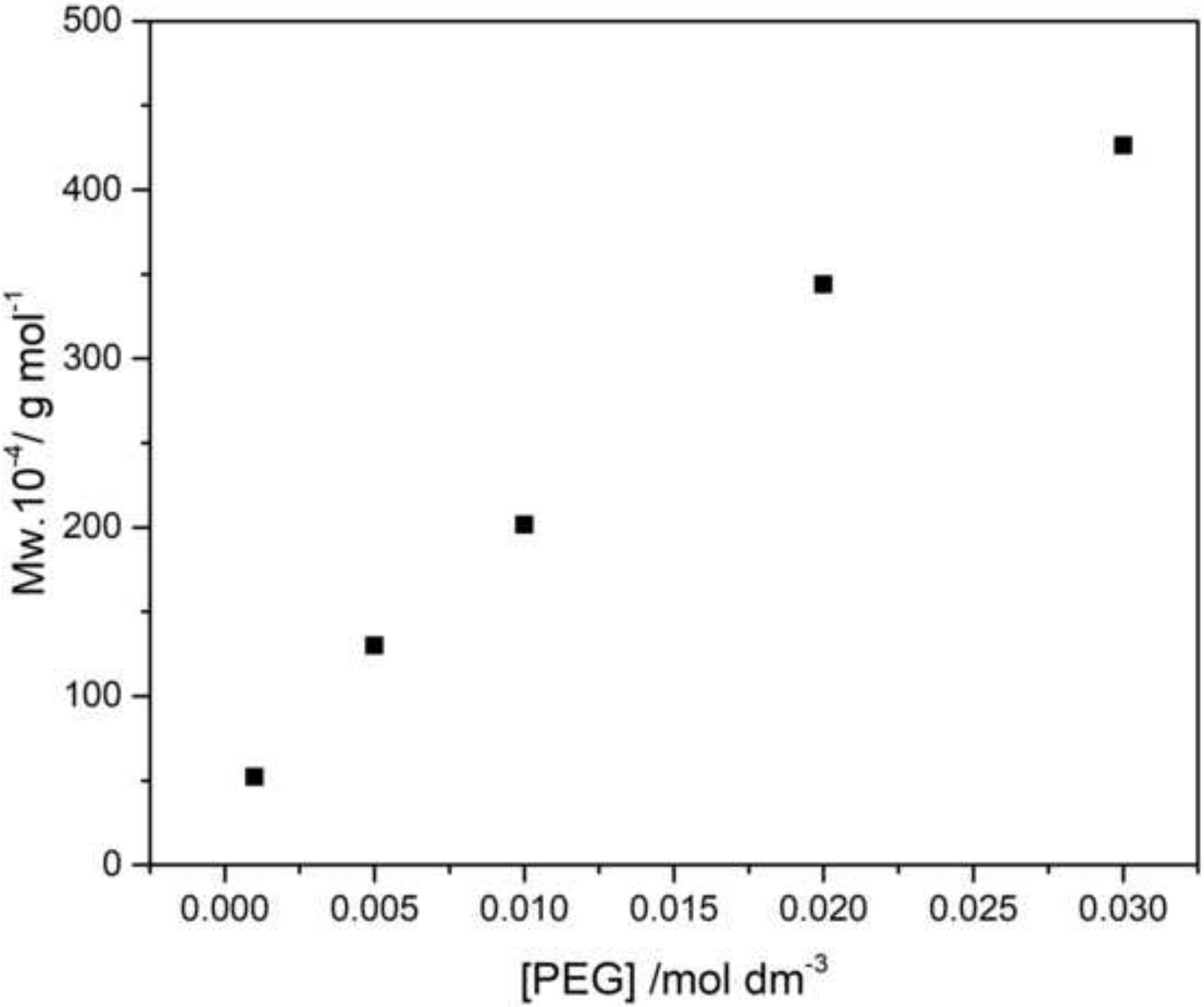
500
400
300
200
100
0
0.000
0.005
0.010
0.015
0.020
0.025
0.030
Mw.10⁻⁴/ g mol⁻¹
[PEG] /mol dm⁻³

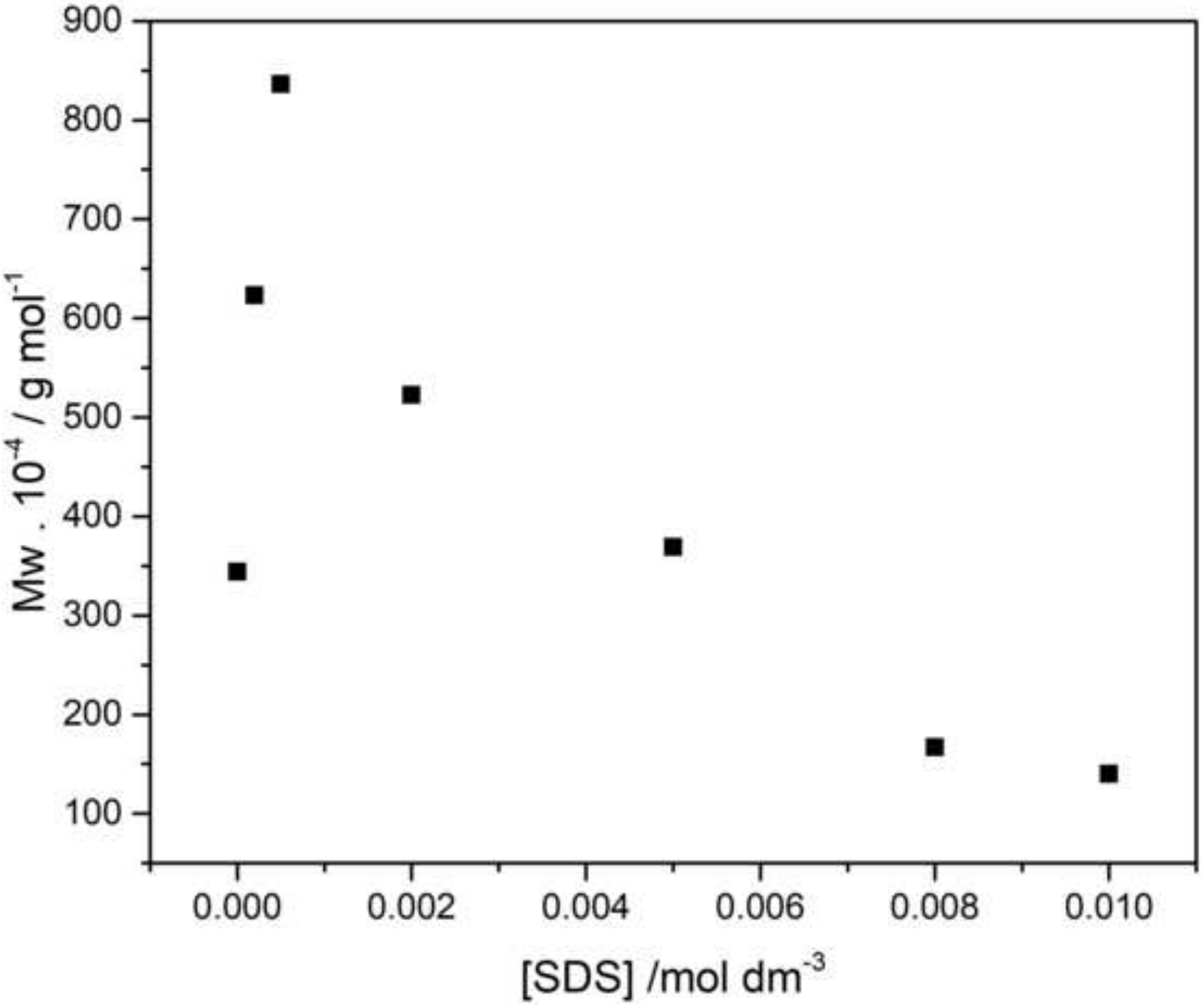
900
800
700
600
500
400
300
200
100
Mw . 10^{-4} / g mol^{-1}
0.000
0.002
0.004
0.006
0.008
0.010
[SDS] /mol dm^{-3}

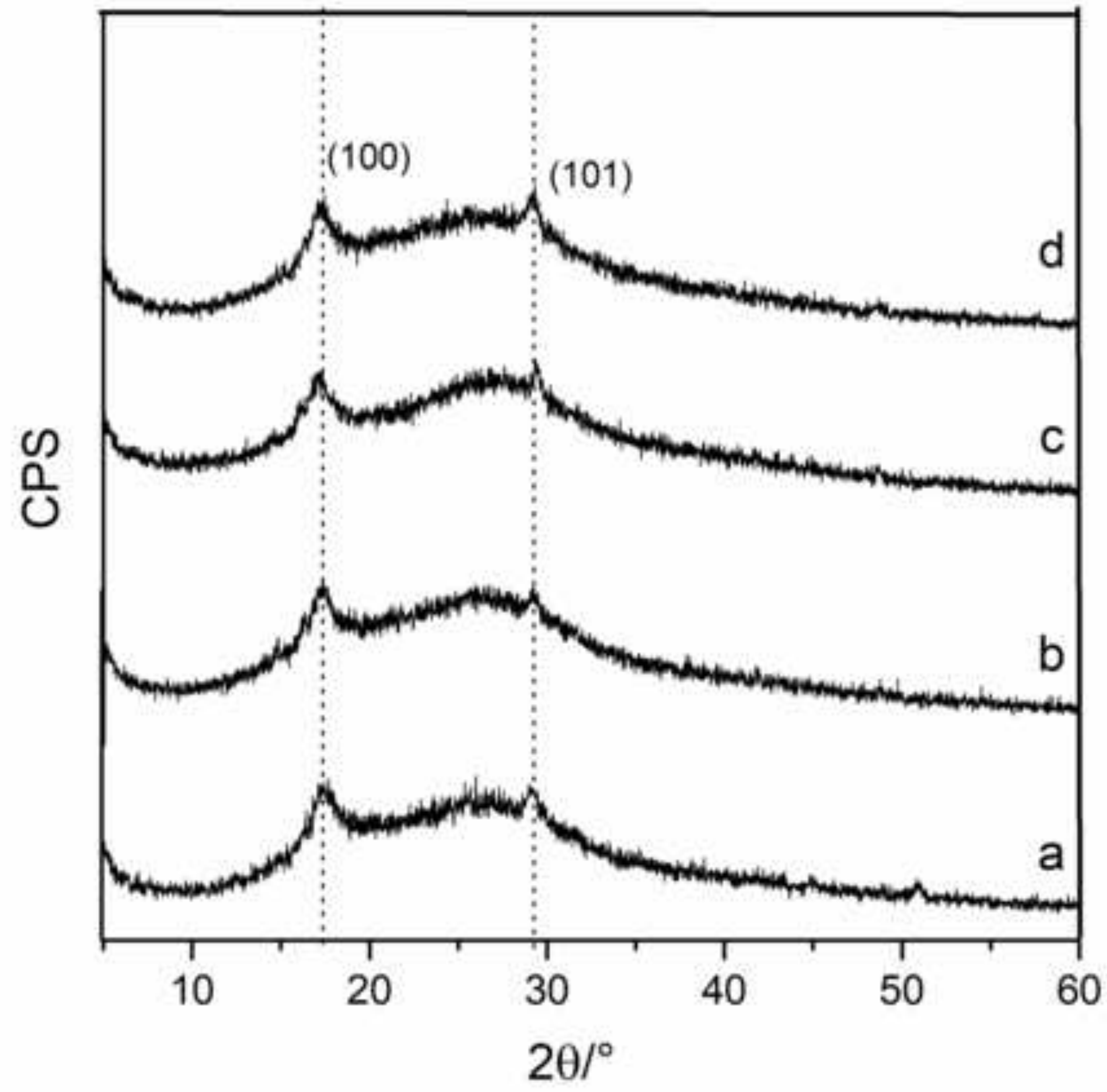
(100)
(101)
d
c
b
a
CPS
10
20
30
40
50
60
2θ/°

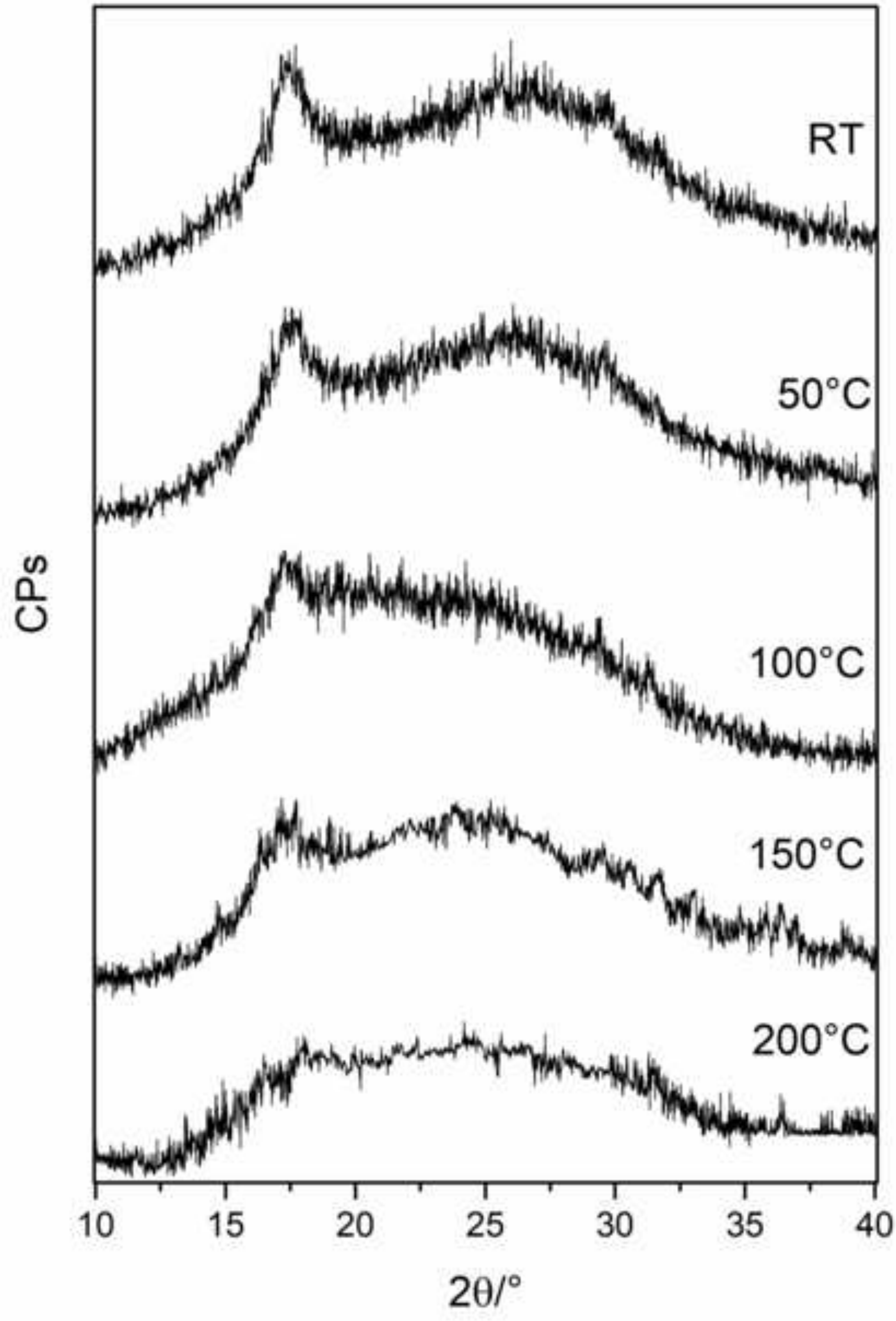
RT
50°C
100°C
150°C
200°C
CPs
10
15
20
25
30
35
40
2θ/°

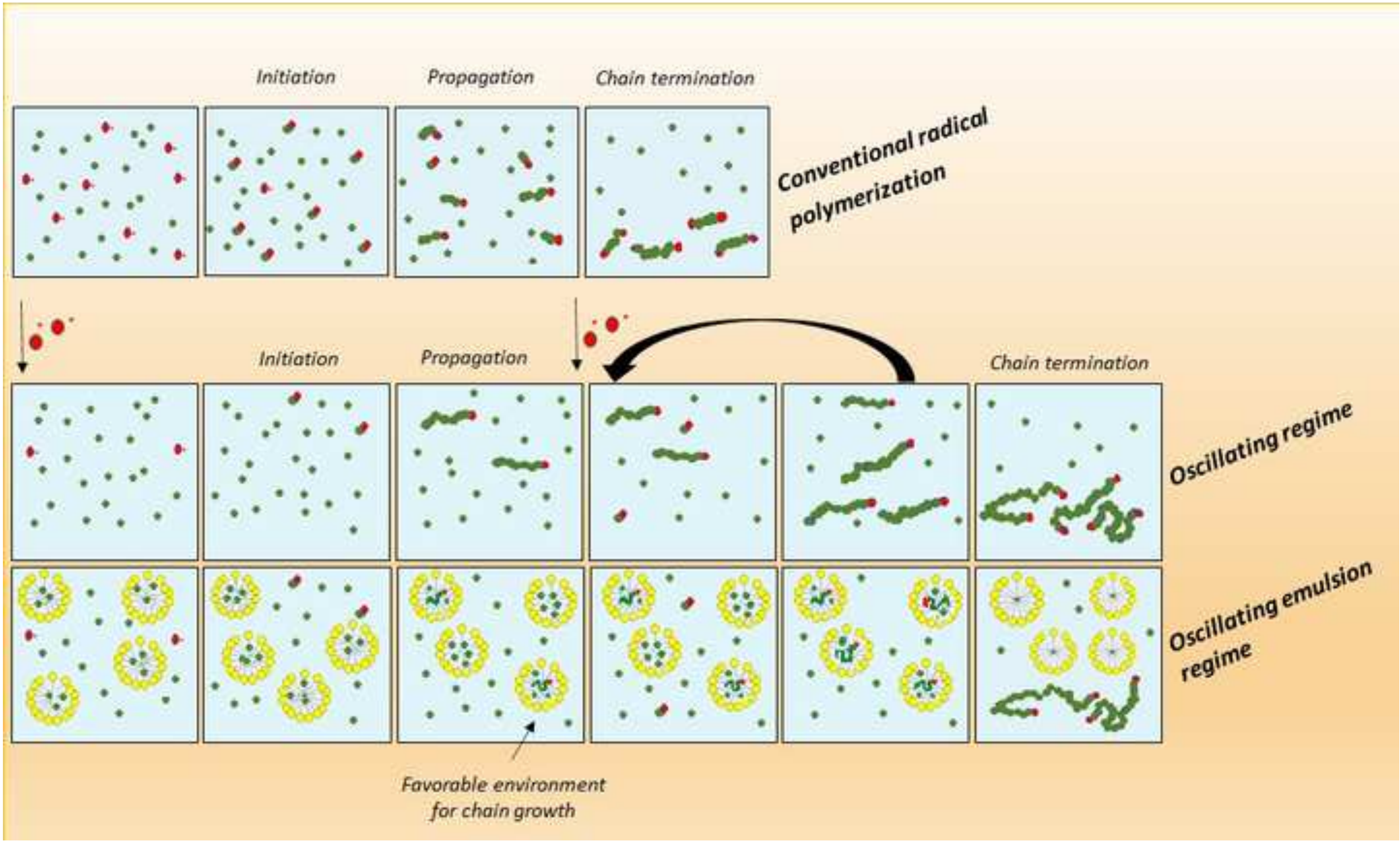
Initiation
Propagation
Chain termination
Conventional radical polymerization
Initiation
Propagation
Chain termination
Oscillating regime
Oscillating emulsion regime
Favorable environment for chain growth